

Differentially Private Heatmaps

Badih Ghazi Junfeng He Kai Kohlhoff Ravi Kumar
 Pasin Manurangsi Vidhya Navalpakkam Nachiappan Valliappan

Google Research
 {badihghazi, ravi.k53}@gmail.com
 {junfenghe, kohlhoff, pasin, vidhyan, nac}@google.com

Abstract

We consider the task of producing heatmaps from users’ aggregated data while protecting their privacy. We give a differentially private (DP) algorithm for this task and demonstrate its advantages over previous algorithms on real-world datasets.

Our core algorithmic primitive is a DP procedure that takes in a set of distributions and produces an output that is close in Earth Mover’s Distance to the average of the inputs. We prove theoretical bounds on the error of our algorithm under a certain sparsity assumption and that these are near-optimal.

1 Introduction

Recently, differential privacy (DP) [DMNS06, DKM⁺06] has emerged as a strong notion of user privacy for data aggregation and machine learning, with practical deployments including the 2022 US Census [Abo18], in industry [EPK14, Sha14, Gre16, App17, DKY17] and in popular machine learning libraries [RE19, TM20]. Over the last few years, DP algorithms have been developed for several analytic tasks involving aggregation of user data.

One of the basic data aggregation tools is a heatmap. Heatmaps are popular for visualizing aggregated data in two or higher dimensions. They are widely used in many fields including computer vision and image processing, spatial data analysis, bioinformatics, etc. Many of these applications involve protecting the privacy of user data. For example, heatmaps for gaze or gene microdata [LXD⁺19, SHHB19] would be based on data from individuals that would be considered private. Similarly, a heatmap of popular locations in a geographic area will be based on user location check-ins, which are sensitive. Motivated by such applications, in this paper, we present an efficient DP algorithm for computing heatmaps with provable guarantees, and evaluate it empirically.

At the core of our algorithm is a primitive solving the following basic task: how to privately aggregate sparse input vectors with a small error as measured by the Earth Mover’s Distance (EMD)? While closely related to heatmaps, the EMD measure is of independent interest: it was originally proposed for computer vision tasks [RTG00] since it matches perceptual similarity better than other measures such as ℓ_1 , ℓ_2 , or KL-divergence [SO95, LB01, WG12]. It is also well-suited for spatial data analysis since it takes the underlying metric space into account and considers “neighboring” bins. EMD is used in spatial analysis [KSS17], human mobility [IBC⁺12], image retrieval [RTG98, PRTB99], face recognition [XYL08], visual tracking [ZYT08], shape matching [GD04], etc. For the task of sparse aggregation under EMD, we give an efficient algorithm with asymptotically tight error. We next describe our results in more detail.

1.1 Our Results

We consider the setting where each user i holds a probability distribution \mathbf{p}_i over points in $[0, 1]^2$, and the goal is to compute the heatmap of the average of these probabilities, i.e., $\frac{1}{n} \sum_{i=1}^n \mathbf{p}_i$. We give an ε -DP algorithm for this task, establish its theoretical guarantees, and provide empirical evaluations of its performance. (For definitions, see Section 2.)

Sparse Aggregation under EMD. At the heart of our approach is the study of aggregation under EMD¹, where we would like to output the estimate of $\frac{1}{n} \sum_{i=1}^n \mathbf{p}_i$ with the error measured in EMD. There are two main reasons why we consider EMD for the error measure. First, a bound on the EMD to the average distribution implies bounds on several metrics commonly used in evaluating heatmaps, including the KL-divergence, ℓ_1 distance, and EMD itself. (We provide more details on this in Appendix B.) Second, while it is possible to obtain DP aggregation algorithms with bounded EMD error, as we will discuss below, any DP aggregation algorithm must suffer errors under other metrics, including KL-divergence or ℓ_1 distance, that grow with the resolution², rendering them impractical when the number of users is small compared to the resolution.

When the distributions \mathbf{p}_i 's are arbitrary, we show that a simple ε -DP algorithm yields a guarantee of $O_\varepsilon(1/\sqrt{n})$ on EMD, and that this bound is essentially optimal. While this is already a reasonable bound, we can improve on it by exploiting a property that is commonly present in distributions used for aggregations: “sparsity” [CPST12].

Following the literature on compressed sensing [IP11, BIRW16], we define our approximation guarantee for the *sparse EMD aggregation* problem with respect to the best k -sparse distribution³ that approximates the average $\mathbf{a} := \frac{1}{n} \sum_{i=1}^n \mathbf{p}_i$ under EMD. More formally, we say that an output distribution $\hat{\mathbf{a}}$ is a (λ, κ) -approximation for sparse EMD aggregation if

$$\text{EMD}(\hat{\mathbf{a}}, \mathbf{a}) \leq \lambda \cdot \min_{k\text{-sparse } \mathbf{a}'} \text{EMD}(\mathbf{a}', \mathbf{a}) + \kappa,$$

where $\lambda, \kappa > 0$ denote the multiplicative approximation ratio and additive error respectively.

Our main algorithmic contribution is in showing that under such a sparse approximation notion, we can achieve an error of only $O_\varepsilon(\sqrt{k}/n)$ and that this is tight.⁴

Theorem 1.1 (Informal). *There exists an ε -DP algorithm that, for any constant $\lambda \in (0, 1)$, can output a $(\lambda, O_\varepsilon(\sqrt{k}/n))$ -approximation for sparse EMD aggregation w.p. 0.99. Furthermore, no ε -DP algorithm can output a $(\lambda, o_\varepsilon(\sqrt{k}/n))$ -approximate solution w.p. 0.1.*

Due to a known connection between sparse EMD aggregation and k -median clustering on the plane [IP11, BIRW16], our result also yields an improved DP algorithm for the latter. We defer the formal statement of our k -median results and discussion to Appendix A.

Experimental results. We test our algorithm on both real-world location datasets and synthetic datasets. The results demonstrate its practicality even for moderate values of $\varepsilon \in [0.5, 5]$ and a number of users equal to 200. Furthermore, we compare our algorithm with simple baselines; under popular metrics for heatmaps, our results demonstrate significant improvements on these regimes of parameters.

¹For a formal definition of EMD, please see Section 2.1.

²Specifically, it follows from previous work [DSS⁺15] that, if we consider the ℓ_1 distance or KL-divergence for $\Delta \times \Delta$ grid and $n \leq O_\varepsilon(\Delta)$, then the error must be $\Omega(1)$.

³A distribution is k -sparse if it is non-zero on at most k points.

⁴Note that the output $\hat{\mathbf{a}}$ need *not* be k -sparse. This is the reason why the approximation ratio λ can be less than one.

1.2 Overview of Techniques

At a high level, our algorithm is largely inspired by the work of [IP11] on *compressed sensing* under EMD. Roughly speaking, in compressed sensing, there is an underlying vector \mathbf{x} that is known to be well-approximated by a sparse vector; we have to provide a matrix \mathbf{A} such that, when we observe the measurements \mathbf{Ax} , we can reconstruct \mathbf{x}' that is close to \mathbf{x} (under a certain metric). This can of course be done trivially by taking \mathbf{A} to, e.g., be the identity matrix. Thus, the objective is to perform this recovery task using as few measurements (i.e., number of rows of \mathbf{A}) as possible. There is a rich literature on compressive sensing; most relevant to our work are the prior papers studying compressive sensing with EMD, in particular, [IP11] and [BIRW16].

[IP11] presented an elegant framework for reducing the compressed sensing problem under EMD to one under ℓ_1 , which is well-studied (see, e.g. [BGI⁺08, BIR08, IR08, BI09]). Their reduction centers around finding a linear transformation with certain properties. Once such a transformation is specified, the algorithm proceeds (roughly) as follows: transform the input \mathbf{x} , run the compressed sensing scheme for ℓ_1 , and “invert” the transformation to get \mathbf{x}' . Note that the number of measurements required is that of the ℓ_1 compressed sensing scheme.

One can try to use the Indyk–Price scheme for DP aggregation by viewing the hidden vector \mathbf{x} as the sum $\sum_{i=1}^n \mathbf{p}_i$, and then adding Laplace noise to each measurement to ensure privacy. Although they did not analyze their guarantees for noisy measurements, one can follow the robustness of known ℓ_1 compressed sensing schemes to analyze the error. Unfortunately, since the error will scale according to the ℓ_1 norm of the noise vector and the noise vector consists of $O(k \cdot \log(n/k))$ entries, this approach only provides an error guarantee of $O(k \cdot (\text{poly } \log n)/n)$.

To overcome this, we observe that, while compressed sensing and DP aggregation seem similar, they have different goals: the former aims to minimize the *number* of measurements whereas the latter aims to minimize the *error* due to the noise added (irrespective of the number of measurements). With this in mind, we proceed by using the Indyk–Price framework but *without compressing*, i.e., we simply measure the entire transformation. Even with this, the noise added to achieve DP is still too large and makes the error dependent on $\log n$. As a final step, to get rid of this factor we carefully select a different noise magnitude for each measurement, which allows us to finally achieve the $O(\sqrt{k})$ error as desired. The details are presented in Section 3.

Our lower bound follows the packing framework of [HT10]. Specifically, we construct a set of k -sparse distributions whose pairwise EMDs are at least $\Omega(1/\sqrt{k})$. The construction is based on an ℓ_1 packing of the $\sqrt{k} \times \sqrt{k}$ grid, which gives a set of size $2^{\Omega(k)}$. It then immediately follows from [HT10] that the error must be at least $\Omega_\epsilon(\sqrt{k}/n)$ with probability 0.9. For more details, see Appendix C

1.3 Related Work and Discussion

In a concurrent and independent work, [BKM⁺22] also study the private heatmaps problem. However, our work differs from theirs in three aspects: (i) they do not formulate the problem in terms of EMD, (ii) their work does not provide any formal utility guarantees unlike ours, (iii) their emphasis is on communication efficiency in distributed/federated setting whereas our focus is more general.

Our DP EMD sparse aggregation algorithm bears high-level similarity to known algorithms for DP hierarchical histograms (see e.g. [CPS⁺12, QYL13]): all algorithms may be viewed as traversing the grid in a top-down manner, starting with larger subgrids and moving on to smaller ones, where a noise is added to the “measurement” corresponding to each subgrid. The differences between the algorithms are in the amount of noise added to each step and how the noisy measurement is used to reconstruct the final output. Our choices of the noise amount and the Indyk–Price reconstruction algorithm are crucial to achieve the optimal EMD error bound stated in Theorem 1.1.

There are also DP hierarchical histogram algorithms that do not fit into the above outline, such as the PrivTree algorithm [ZXX16]. An advantage of our approach is that the only aggregation primitive required is the Laplace mechanism; therefore, while we focus on the *central* model of DP (where the analyzer can see the raw input and only the output is required to be DP), our algorithm extends naturally to distributed models that can implement the Laplace mechanism, including the secure aggregation model and the shuffle model [BBGN20, GMPV20]. On the other hand, algorithms such as PrivTree that use more complicated primitives cannot be easily implemented in these models.

2 Notation and Preliminaries

For $N \in \mathbb{N} \cup \{0\}$, we write $[N]$ to denote $\{0, \dots, N\}$. Let G_Δ be the set of $(\Delta \times \Delta)$ grid points in $[0, 1)^2$; specifically, $G_\Delta = \{(i/\Delta, j/\Delta) \mid i, j \in [\Delta - 1]\}$. For notational convenience, we assume throughout that $\Delta = 2^\ell$ for some $\ell \in \mathbb{N}$.

For an index set \mathcal{I} , we view $\mathbf{p} \in \mathbb{R}^\mathcal{I}$ as a vector indexed by \mathcal{I} and we write $\mathbf{p}(i)$ to denote the value of its i th coordinate; this notation extends naturally to the set $S \subseteq \mathcal{I}$ of coordinates, for which we let $\mathbf{p}(S) := \sum_{i \in S} \mathbf{p}(i)$. Furthermore, we use $\mathbf{p}|_S$ to denote the restriction of \mathbf{p} to S ; more formally, $\mathbf{p}|_S(i) = \mathbf{p}(i)$ if $i \in S$ and $\mathbf{p}|_S(i) = 0$ otherwise. We also write $\mathbf{p}|_{\bar{S}}$ as a shorthand for $\mathbf{p} - \mathbf{p}|_S$, i.e., the restriction of \mathbf{p} to the complement of S . We use $\text{supp}(\mathbf{p})$ to denote the set of non-zero coordinates of vector \mathbf{p} . A vector is said to be k -sparse if its support is of size at most k . Recall that the ℓ_1 -norm of a vector $\mathbf{p} \in \mathbb{R}^\mathcal{I}$ is $\|\mathbf{p}\|_1 := \sum_{i \in \mathcal{I}} |\mathbf{p}(i)|$.

2.1 Earth Mover's Distance (EMD)

Given two non-negative vectors $\mathbf{p}, \mathbf{q} \in \mathbb{R}_{\geq 0}^{G_\Delta}$ such that $\|\mathbf{p}\|_1 = \|\mathbf{q}\|_1$, their *Earth Mover's Distance* (EMD) is

$$\text{EMD}(\mathbf{p}, \mathbf{q}) := \min_\gamma \sum_{x \in G_\Delta} \sum_{y \in G_\Delta} \gamma(x, y) \cdot \|x - y\|_1,$$

where the minimum is over $\gamma \in \mathbb{R}_{\geq 0}^{G_\Delta \times G_\Delta}$ whose marginals are \mathbf{p} and \mathbf{q} . (I.e., for all $x \in G_\Delta$, $\sum_{y \in G_\Delta} \gamma(x, y) = \mathbf{p}(x)$ and, for all $y \in G_\Delta$, $\sum_{x \in G_\Delta} \gamma(x, y) = \mathbf{q}(y)$.)

We define the *EMD norm* of a vector $\mathbf{w} \in \mathbb{R}^{G_\Delta}$ by

$$\|\mathbf{w}\|_{\text{EMD}} := \min_{\substack{\mathbf{p}, \mathbf{q} \in \mathbb{R}_{\geq 0}^{G_\Delta} \\ \mathbf{p} - \mathbf{q} + \mathbf{r} = \mathbf{w}, \|\mathbf{p}\|_1 = \|\mathbf{q}\|_1}} \text{EMD}(\mathbf{p}, \mathbf{q}) + \alpha \cdot \|\mathbf{r}\|,$$

where $\alpha = 2$ is the diameter of our space $[0, 1) \times [0, 1)$.

The following simple lemma will be useful when dealing with unnormalized vs normalized vectors.

Lemma 2.1. *Suppose that $\mathbf{s}, \hat{\mathbf{s}} \in \mathbb{R}_{\geq 0}^{G_\Delta}$ are such that $\|\mathbf{s}\|_1 = n$ and $\|\mathbf{s} - \hat{\mathbf{s}}\|_{\text{EMD}} \leq n/2$. Let $\mathbf{a} = \mathbf{s}/\|\mathbf{s}\|_1$ and $\hat{\mathbf{a}} = \hat{\mathbf{s}}/\|\hat{\mathbf{s}}\|_1$. Then, we have $\|\mathbf{a} - \hat{\mathbf{a}}\|_{\text{EMD}} \leq 4\|\mathbf{s} - \hat{\mathbf{s}}\|_{\text{EMD}}/n$.*

Proof. Let $\zeta = \|\mathbf{s} - \hat{\mathbf{s}}\|_{\text{EMD}}$; observe that $|\|\mathbf{s}\|_1 - \|\hat{\mathbf{s}}\|_1| \geq \zeta$. As a result, we have $\|\hat{\mathbf{s}}\|_1 \in [n - \zeta, n + \zeta]$. Thus,

$$\begin{aligned} \|\hat{\mathbf{s}}/n - \hat{\mathbf{a}}\|_{\text{EMD}} &\leq \|\hat{\mathbf{s}}\|_{\text{EMD}} \cdot \left| \frac{1}{n} - \frac{1}{\|\hat{\mathbf{s}}\|_1} \right| \\ &\leq (n + \zeta) \cdot \left| \frac{1}{n} - \frac{1}{n - \zeta} \right| \leq \frac{3\zeta}{n}. \end{aligned}$$

As a result, from the triangle inequality, we have

$$\begin{aligned} \|\mathbf{a} - \hat{\mathbf{a}}\|_{\text{EMD}} &\leq \|\mathbf{a} - \hat{\mathbf{s}}/n\|_{\text{EMD}} + \|\hat{\mathbf{s}}/n - \hat{\mathbf{a}}\|_{\text{EMD}} \\ &\leq \frac{\zeta}{n} + \frac{3\zeta}{n} = \frac{4\zeta}{n}. \end{aligned} \quad \square$$

2.2 Differential Privacy

Two input datasets \mathbf{X}, \mathbf{X}' are *neighbors* if \mathbf{X}' results from adding or removing a single user's data from \mathbf{X} . In our setting, each user i 's data is a distribution \mathbf{p}_i over G_Δ .

Definition 2.1 (Differential Privacy; [DMNS06]). A mechanism \mathcal{M} is said to be ε -DP iff, for every set O of outputs and every pair \mathbf{X}, \mathbf{X}' of neighboring datasets, $\Pr[\mathcal{M}(\mathbf{X}) \in O] \leq e^\varepsilon \cdot \Pr[\mathcal{M}(\mathbf{X}') \in O]$.

For a vector-valued function f , its ℓ_1 -sensitivity, denoted by $S_1(f)$, is defined as $\max_{\text{neighbors } \mathbf{X}, \mathbf{X}'} \|f(\mathbf{X}) - f(\mathbf{X}')\|_1$.

Definition 2.2 (Laplace Mechanism). The *Laplace mechanism* with parameter $b > 0$ adds an independent noise drawn from the Laplace distribution $\text{Lap}(b)$ to each coordinate of a vector-valued function f .

Lemma 2.2 ([DMNS06]). *The Laplace mechanism with parameter $S_1(f)/\varepsilon$ is ε -DP.*

2.3 Heatmaps

Given $\mathbf{p} \in \mathbb{R}_{\geq 0}^{G_\Delta}$, its associated *heatmap* with Gaussian filter variance σ^2 is defined as

$$H_{\mathbf{p}}^\sigma(x, y) = \sum_{(x', y') \in G_\Delta} \frac{1}{Z(x', y')} e^{-\frac{(x-x')^2 + (y-y')^2}{2\sigma^2}} \cdot p(x', y')$$

for all $(x, y) \in G_\Delta$, where $Z(x', y') := \sum_{(x'', y'') \in G_\Delta} e^{-\frac{(x-x'')^2 + (y-y'')^2}{2\sigma^2}}$ is the normalization factor.

In the heatmap aggregation problem over n users, each user i has a probability distribution \mathbf{p}_i over G_Δ . The goal is to output an estimate of the aggregated heatmap $H_{\mathbf{a}}^\sigma$ where $\mathbf{a} = \frac{1}{n} \sum_{i \in [n]} \mathbf{p}_i$.

3 Algorithm

In this section, we describe our private sparse EMD aggregation algorithm and prove our main result.

Theorem 3.1. *For any $\varepsilon > 0$ and $\lambda \in (0, 1)$, there is an ε -DP algorithm that can, w.p. 0.99, output a $\left(\lambda, O\left(\frac{\sqrt{k}}{\lambda \varepsilon n}\right)\right)$ -approximation for the k -sparse EMD aggregation problem.*

3.1 Pyramidal Transform

As alluded to in Section 1, we use a linear transformation from [IP11]. This linear transformation is the so-called (*scaled*) *pyramidal transform*, whose variant is also often used in (metric) embedding of EMD to ℓ_1 [Cha02, IT03]. Roughly speaking, the transform represents a hierarchical partitioning of $[0, 1]^2$ into subgrids, where a subgrid at a level is divided into four equal subgrids at the next level. The (scaled) pyramidal transform has one row corresponding to each subgrid; the row is equal to the indicator vector of the subgrid scaled by its side length. These are formalized below.

Algorithm 1 DPSPARSEEMDAGG

- 1: **Input:** distributions $\mathbf{p}_1, \dots, \mathbf{p}_n$ on G_Δ
- 2: **Parameters:** $\varepsilon_1, \dots, \varepsilon_\ell > 0, w \in \mathbb{N}$
- 3: $\mathbf{s} \leftarrow \sum_{i=1}^n \mathbf{p}_i$
- 4: **for** $i = 0, \dots, \ell$ **do**
- 5: $\nu_i \leftarrow \text{Lap}(1/\varepsilon_i)^{\otimes m_i}$
- 6: $\mathbf{y}'_i \leftarrow \frac{1}{2^i} (\mathbf{P}_i \mathbf{s} + \nu_i)$
- 7: **end for**
- 8: $\mathbf{y}' \leftarrow [\mathbf{y}'_0 \cdots \mathbf{y}'_\ell]$
- 9: $\hat{\mathbf{s}} \leftarrow \text{RECONSTRUCT}(\mathbf{y}'; w)$
- 10: **return** $\hat{\mathbf{a}} := \hat{\mathbf{s}} / \|\hat{\mathbf{s}}\|$

Algorithm 2 RECONSTRUCT

- 1: **Input:** noisy measurements $\mathbf{y}' \in \mathbb{R}^{\bigcup_{i \in [\ell]} C_{2^i}}$
- 2: **Parameters:** $w \in \mathbb{N}$
- 3: $S_0 \leftarrow C_1$
- 4: **for** $i = 1, \dots, \ell$ **do**
- 5: $T_i \leftarrow \text{children}(S_{i-1})$
- 6: $S_i \leftarrow$ the set of $\min\{w, |T_i|\}$ coordinates in T_i with maximum values in \mathbf{y}'
- 7: **end for**
- 8: $S \leftarrow \bigcup_{i \in [\ell]} S_i$ and $\hat{\mathbf{y}} \leftarrow \mathbf{y}'|_S$
- 9: **return** $\hat{\mathbf{s}} \leftarrow \arg \min_{\mathbf{s}' \geq \mathbf{0}} \|\hat{\mathbf{y}} - \mathbf{P}\mathbf{s}'\|_1$

Definition 3.1. For $i \in \mathbb{N} \cup \{0\}$, we let C_{2^i} denote the set of *level i grid cells* defined as $C_{2^i} := \{[a, a + 2^{-i}] \times [b, b + 2^{-i}] \mid (a, b) \in G_{2^i}\}$; let $m_i := |C_{2^i}|$.

For $i \in [\ell]$, the *level- i grid partition map* is defined as the matrix $\mathbf{P}_i \in \{0, 1\}^{C_{2^i} \times G_\Delta}$ where $\mathbf{P}_i(c, p) = 1$ iff $p \in c$. The (*scaled*) *pyramidal transform* is the matrix $\mathbf{P} \in \mathbb{R}^{\bigcup_{i=0}^\ell C_{2^i} \times G_\Delta}$ defined by

$$\mathbf{P} := [\mathbf{P}_0^\top \ 2^{-1}\mathbf{P}_1^\top \ \dots \ 2^{-\ell}\mathbf{P}_\ell^\top]^\top.$$

3.2 The Algorithm

Our algorithm for sparse EMD aggregation consists of two components. The first component (Algorithm 1) aggregates the input distributions (Line 3) and applies the pyramidal transform to the aggregate, adding different amounts of Laplace noise for different levels of the grid (Lines 5, 6). (The parameters $\varepsilon_1, \dots, \varepsilon_\ell$, which govern the amount of Laplace noise, will be specified in the next subsection.) The second component (Algorithm 2) takes these noisy measurements for every level of the grid and reconstructs the solution by first recovering the ℓ_1 solution (Line 8) and then the EMD solution using a linear program (Line 9).

We stress that our algorithm is similar to that of [IP11] except for two points: first, we add noise to the measurements and, second, we are not doing any “compression” in contrast to [IP11], which takes a wide matrix \mathbf{A} for ℓ_1 recovery and multiplies it with $\mathbf{P}\mathbf{s}$.

3.3 Analysis

Following the framework of [IP11], our analysis proceeds in two stages. We first show that the “recovered” $\hat{\mathbf{y}}$ is close, in the ℓ_1 metric, to the true value of $\mathbf{P}\mathbf{s}$. Then, we use the properties of \mathbf{P} to argue that the output $\hat{\mathbf{s}}$ is close, in EMD, to \mathbf{s} . Since we are adding noise to our measurement, we need to extend the work of [IP11] to be robust to noise. Finally, we set the privacy parameters $\varepsilon_1, \dots, \varepsilon_\ell$ to finish our proof of Theorem 3.1.

Let us now briefly demystify the additive error bound $O_{\varepsilon, \lambda}(\sqrt{k})$ that we end up with for $\hat{\mathbf{s}}$ (which ultimately gives the $O_{\varepsilon, \lambda}(\sqrt{k}/n)$ error bound for the normalized $\hat{\mathbf{a}}$). We will select $w = O_\lambda(k)$ so as to have an additive error of $O_\varepsilon(\sqrt{w})$. At a high level, each noise $\frac{1}{2^i} \cdot \nu_i(t)$ added to a “queried” term $\mathbf{y}_i(t)$ for $t \in T_i$ permeates to an error of the same order. For simplicity, assume for the moment that $|\nu_i(t)| = O(1/\varepsilon_i)$. Now, notice that if we are at level $i < \log \sqrt{w}$, then $|T_i| = |C_{2^i}| = 2^{2i}$ and thus the total error contribution of this level is $O(2^i/\varepsilon_i)$. On the other hand, for a level $i \geq \log \sqrt{w}$, we will have $|T_i| = w$ and the error contribution is $O\left(\frac{w}{2^i \varepsilon_i}\right)$. Now, when $i = \log \sqrt{w} \pm O(1)$, these error terms are $O(\sqrt{w}/\varepsilon_i)$ and thus we should set $\varepsilon_i = \Omega(1)$ to get the desired bound. However, in terms of $|i - \log \sqrt{w}|$, these error

terms become exponentially smaller, i.e., $O\left(\frac{\sqrt{w}}{2^{|i-\log\sqrt{w}|\varepsilon_i}}\right)$. This leads to the natural choices of ε_i we use, which is to make it proportional to $\gamma^{|i-\log\sqrt{w}|}$ for some constant $\gamma > 0.5$. This indeed leads to the desired $O_\varepsilon(\sqrt{w}) = O_{\varepsilon,\lambda}(\sqrt{k})$ bound.

Phase I: ℓ_1 Recovery. We will now analyze the ℓ_1 recovery guarantee of $\hat{\mathbf{y}}$. Our recovery algorithm, which is an adaptation of [IP11], does *not* work for general hidden vectors. However, it works well for those that follow a certain “tree-like structure”, formalized below.

Definition 3.2 ([IP11]). For $i \geq 1$, a grid cell $c' \in C_{2^i}$ is said to be a *child* of grid cell $c \in C_{2^{i-1}}$ if $c \subseteq c'$. This forms a tree rooted at $[0, 1) \times [0, 1) \in C_0$ where every internal node has exactly four children. We let \mathcal{T}_w denote the set of all trees such that the number of nodes at each level is at most w .

Let \mathcal{M}_w denote the set of $\mathbf{y} = [\mathbf{y}_0 \cdots \mathbf{y}_\ell]$ where $\mathbf{y}_i \in \mathbb{R}_{\geq 0}^{C_{2^i}}$ such that

1. $\text{supp}(\mathbf{y}) \subseteq T$ for some tree $T \in \mathcal{T}_w$.
2. For all $i \in [\ell - 1], p \in C_{2^i}$, the following holds: $\mathbf{y}(p) \geq 2 \cdot \mathbf{y}(\text{children}(p))$.

Under the above notion, we can adapt the ℓ_1 recovery analysis of [IP11] in the no-noise case to our regime, where the noise shows up as an error:

Lemma 3.2. Let $\mathbf{y}^* \in \arg \min_{\mathbf{y} \in \mathcal{M}_w} \|\mathbf{P}\mathbf{s} - \mathbf{y}\|_1$ where $\text{supp}(\mathbf{y}^*) \subseteq T^*$ for some $T^* \in \mathcal{T}_w$; let T_i^* denote $T^* \cap C_{2^i}$ and $V_i = T_i^* \setminus S_i$ for all $i \in [\ell]$. Then, $\hat{\mathbf{y}}$ on Line 8 of RECONSTRUCT satisfies $\|\hat{\mathbf{y}} - \mathbf{P}\mathbf{s}\|_1 \leq 3\|\mathbf{y}^* - \mathbf{P}\mathbf{s}\|_1 + O\left(\sum_{i \in [\ell]} \frac{1}{2^i} \|\nu_i|_{V_i \cup S_i}\|_1\right)$.

Proof. For every $q \in T^* \setminus S$, let $R(q)$ be the highest ancestor of q that does not belong to S . We have

$$\begin{aligned} \|\mathbf{y}^*|_{\bar{S}}\|_1 &= \sum_{q \in T^* \setminus S} \mathbf{y}^*(q) = \sum_{i \in [\ell]} \sum_{p \in V_i} \sum_{q \in R^{-1}(p)} \mathbf{y}^*(q) \\ &\stackrel{(\diamond)}{\leq} \sum_{i \in [\ell]} \sum_{p \in V_i} 2\mathbf{y}^*(p) = 2 \sum_{i \in [\ell]} \mathbf{y}^*(V_i), \end{aligned} \tag{1}$$

where (\diamond) follows from the second property of \mathcal{M}_w .

Next, consider the algorithm at the i th iteration and $p \in V_i$. Since p was not picked, the following must hold for all $q \in S_i \setminus T_i^*$: $\mathbf{y}'(p) \leq \mathbf{y}'(q)$. Observe also that from $|S_i| = \max\{w, |C_{2^i}|\}$ and $|T_i^*| \leq \max\{w, |C_{2^i}|\}$, we also have $|S_i \setminus T_i^*| \geq |T_i^* \setminus S_i| = |V_i|$. Thus, we get

$$\mathbf{y}'(V_i) \leq \mathbf{y}'(S_i \setminus T_i^*). \tag{2}$$

From this and (1), we can further derive

$$\begin{aligned} &\|\mathbf{y}^*|_{\bar{S}}\|_1 \\ &\stackrel{(1)}{\leq} 2 \left(\sum_{i \in [\ell]} (\mathbf{y}^*(V_i) - \mathbf{P}\mathbf{s}(V_i)) + \mathbf{P}\mathbf{s}(S_i \setminus T_i^*) \right) \\ &\quad + \left(\sum_{i \in [\ell]} \mathbf{P}\mathbf{s}(V_i) - \mathbf{P}\mathbf{s}((S_i \setminus T_i^*)) \right) \\ &\stackrel{(\square)}{\leq} 2\|\mathbf{y}^* - \mathbf{P}\mathbf{s}\|_1 + 2 \left(\sum_{i \in [\ell]} \mathbf{P}\mathbf{s}(V_i) - \mathbf{P}\mathbf{s}((S_i \setminus T_i^*)) \right) \end{aligned}$$

$$\begin{aligned}
& \stackrel{(\Delta)}{\leq} 2\|\mathbf{y}^* - \mathbf{P}\mathbf{s}\|_1 + 2 \left(\sum_{i \in [\ell]} \frac{1}{2^i} \|\nu_i|_{V_i \cup (S_i \setminus T_i^*)}\|_1 \right) \\
& \quad + 2 \left(\sum_{i \in [\ell]} \mathbf{y}'(V_i) - \mathbf{y}'((S_i \setminus T_i^*)) \right) \\
& \stackrel{(2)}{\leq} 2\|\mathbf{y}^* - \mathbf{P}\mathbf{s}\|_1 + 2 \left(\sum_{i \in [\ell]} \frac{1}{2^i} \|\nu_i|_{V_i \cup (S_i \setminus T_i^*)}\|_1 \right), \tag{3}
\end{aligned}$$

where (\square) follows from $\text{supp}(\mathbf{y}^*) \subseteq T^* = \bigcup_{i \in [\ell]} T_i^*$ and (Δ) follows from how \mathbf{y}' is calculated. Finally, from $\hat{\mathbf{y}} = \mathbf{y}'|_S$ and how each entry of \mathbf{y}' is computed, we have

$$\begin{aligned}
\|\hat{\mathbf{y}} - \mathbf{P}\mathbf{s}\|_1 &= \|\mathbf{y}'|_S - \mathbf{P}\mathbf{s}|_S\|_1 + \|\mathbf{P}\mathbf{s}_{\bar{S}}\|_1 \\
&\leq \left(\sum_{i \in [\ell]} \frac{1}{2^i} \|\nu_i|_{S_i}\|_1 \right) + \|\mathbf{y}^*|_{\bar{S}}\|_1 + \|\mathbf{y}^*|_{\bar{S}} - \mathbf{P}\mathbf{s}|_{\bar{S}}\|_1 \\
&\stackrel{(3)}{\leq} \left(\sum_{i \in [\ell]} \frac{1}{2^i} \|\nu_i|_{S_i}\|_1 \right) \\
& \quad + \left(2\|\mathbf{y}^* - \mathbf{P}\mathbf{s}\|_1 + 2 \left(\sum_{i \in [\ell]} \frac{1}{2^i} \|\nu_i|_{V_i \cup (S_i \setminus T_i^*)}\|_1 \right) \right) \\
& \quad + \|\mathbf{y}^* - \mathbf{P}\mathbf{s}\|_1 \\
&\leq 3\|\mathbf{y}^* - \mathbf{P}\mathbf{s}\|_1 + 3 \left(\sum_{i \in [\ell]} \frac{1}{2^i} \|\nu_i|_{V_i \cup S_i}\|_1 \right). \quad \square
\end{aligned}$$

Phase II: From ℓ_1 to EMD. We now proceed to bound the EMD error. The main lemma is stated below.

Lemma 3.3. *Let the notation be as in Lemma 3.2. For any $\eta' \in (0, 1)$, by setting $w = O(k/(\eta')^2)$, the output $\hat{\mathbf{s}}$ of RECONSTRUCT satisfies $\|\mathbf{s} - \mathbf{s}^*\|_{\text{EMD}} \leq \eta' \cdot \min_{k\text{-sparse } \mathbf{s}'} \|\mathbf{s} - \mathbf{s}'\|_{\text{EMD}} + O\left(\sum_{i \in [\ell]} \frac{1}{2^i} \|\nu_i|_{V_i \cup S_i}\|_1\right)$.*

Similar to the proof of [IP11], our proof of Lemma 3.3 converts the recovery guarantee under ℓ_1 metric to that under EMD; to do this, we need the following two statements from prior work.

Lemma 3.4 (Model-Alignment of EMD with \mathcal{M}_w [IP11]). *For any $\mathbf{x} \in \mathbb{R}_{\geq 0}^{G_\Delta}$, $k \in \mathbb{N}$ and $\eta \in (0, 1)$, there exist $w = O(k/\eta^2)$ and $\mathbf{y}^* \in \mathcal{M}_w$ such that $\|\mathbf{y}^* - \mathbf{P}\mathbf{s}\|_1 \leq \eta \cdot \min_{k\text{-sparse } \mathbf{x}'} \|\mathbf{x} - \mathbf{x}'\|_{\text{EMD}}$.*

Lemma 3.5 (EMD-to- ℓ_1 Expansion [IT03]). *For all $\mathbf{z} \in \mathbb{R}^{G_\Delta}$, $\|\mathbf{z}\|_{\text{EMD}} \leq \|\mathbf{P}\mathbf{z}\|_1$.*

Proof of Lemma 3.3. Recall that we use \mathbf{s} to denote the true sum $\sum_{i=1}^n \mathbf{p}_i$. We set $\eta = \eta'/6$ and let $w = O(k/\eta^2) = O(k/(\eta')^2)$ be as in Lemma 3.4, which ensures that there exists $\mathbf{y}^* \in \mathcal{M}_w$ with

$$\|\mathbf{y}^* - \mathbf{P}\mathbf{s}\|_1 \leq \eta \cdot \min_{k\text{-sparse } \mathbf{s}'} \|\mathbf{s} - \mathbf{s}'\|_{\text{EMD}}. \tag{4}$$

Thus, using Lemma 3.5, we can derive

$$\|\mathbf{s} - \mathbf{s}^*\|_{\text{EMD}} \leq \|\mathbf{P}(\mathbf{s} - \mathbf{s}^*)\|_1$$

$$\begin{aligned}
& \text{(triangle inequality)} \leq \|\hat{\mathbf{y}} - \mathbf{P}\mathbf{s}\|_1 + \|\hat{\mathbf{y}} - \mathbf{P}\mathbf{s}^*\|_1 \\
& \text{(how } \mathbf{s}^* \text{ is computed)} \leq 2\|\hat{\mathbf{y}} - \mathbf{P}\mathbf{s}\|_1 \\
& \text{(Lemma 3.2)} \leq 6\|\mathbf{y}^* - \mathbf{P}\mathbf{s}\|_1 \\
& \quad + O\left(\sum_{i \in [\ell]} \frac{1}{2^i} \|\nu_i|_{V_i \cup S_i}\|_1\right) \\
& \stackrel{(4)}{\leq} \eta' \cdot \min_{k\text{-sparse } \mathbf{s}'} \|\mathbf{s} - \mathbf{s}'\|_{\text{EMD}} \\
& \quad + O\left(\sum_{i \in [\ell]} \frac{1}{2^i} \|\nu_i|_{V_i \cup S_i}\|_1\right). \quad \square
\end{aligned}$$

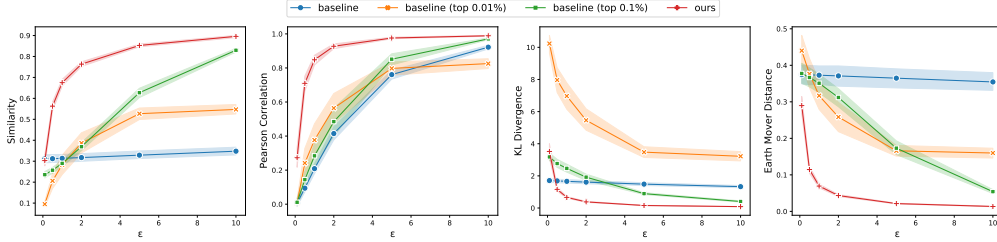


Figure 1: Metrics averaged over 60 runs when varying ϵ . Shaded areas indicate 95% confidence interval.

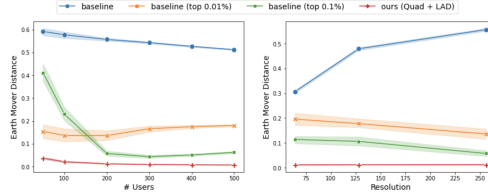


Figure 2: Effect of the #users and grid resolution on EMD.

Finishing the Proof. We now select the privacy parameters and complete the proof of Theorem 3.1.

Proof of Theorem 3.1. Let $w = O(k/(\eta')^2)$ be as in Lemma 3.3 with $\eta' = \lambda/4$, and let $q = \lfloor \log_2 \sqrt{w} \rfloor$. Let $\gamma = 0.8$ be the “decay rate” for ϵ_i 's, and let $Z = \sum_{i=0}^{\ell} \gamma^{|i-q|} \leq O(1)$ be the normalization factor. We run Algorithm 1 with $\epsilon_i = \gamma^{|i-q|} \cdot \epsilon/Z$.

Privacy Analysis. We can view the i th iteration of the algorithm as releasing $2^i \mathbf{y}'_i = \mathbf{P}_i \mathbf{s} + \nu_i$. Since each \mathbf{p}_i has ℓ_1 norm at most one, its sensitivity with respect to $\mathbf{P}_i \mathbf{s}$ is at most one; thus, Lemma 2.2 implies that the i th iteration is ϵ_i -DP. As a result, by basic composition theorem of DP, we can conclude that releasing all of $\mathbf{y}'_0, \dots, \mathbf{y}'_{\ell}$ is $(\epsilon_0 + \dots + \epsilon_{\ell})$ -DP. Since the reconstruction is simply a post-processing step, the post-processing property of DP ensures that Algorithm 1 is $(\epsilon_0 + \dots + \epsilon_{\ell})$ -DP. Finally, observe that by definition of ϵ_i 's, we have $\epsilon_0 + \dots + \epsilon_{\ell} = \epsilon$ as desired.

Utility Analysis. Applying Lemma 3.3, we can conclude that $\|\mathbf{s} - \mathbf{s}^*\|_{\text{EMD}} \leq \eta' \cdot \min_{k\text{-sparse } \mathbf{s}'} \|\mathbf{s} - \mathbf{s}'\|_{\text{EMD}} + \xi$, where $\xi = O\left(\sum_{i \in [\ell]} \frac{1}{2^i} \|\nu_i\|_{V_i \cup S_i}\right)$. Recall that each of V_i, S_i 's is of size at most $\max\{w, 2^{2i}\}$ (because of definition of \mathcal{M}_w and the fact that $m_i = |C_{2^i}| = 2^{2i}$), and that each entry of ν_i is sampled from $\text{Lap}(1/\varepsilon_i)$. As a result, we have

$$\begin{aligned} \mathbb{E}[\xi] &\leq O\left(\sum_{i \in [\ell]} \frac{1}{2^i} \cdot \max\{w, 2^{2i}\} \cdot \frac{1}{\varepsilon_i}\right) \\ &= O\left(\sum_{i \in [q]} \frac{2^i}{\gamma^{q-i}\varepsilon}\right) + O\left(\sum_{i \in \{q+1, \dots, \ell\}} \frac{k}{\lambda^2} \cdot \frac{1}{2^i \gamma^{i-q}\varepsilon}\right) \\ &= O\left(\frac{2^q}{\varepsilon}\right) + O\left(\frac{k}{\lambda^2} \cdot \frac{1}{2^q} \cdot \frac{1}{\varepsilon}\right) = O\left(\frac{\sqrt{k}}{\lambda\varepsilon}\right), \end{aligned}$$

where the last bound follows from our choice of $\gamma > 0.5$ and $q = \lfloor \log_2 \sqrt{w} \rfloor$. Hence, by Markov's inequality, w.p. 0.99, we have $\|\mathbf{s} - \mathbf{s}^*\|_{\text{EMD}} \leq \eta' \cdot \min_{k\text{-sparse } \mathbf{s}'} \|\mathbf{s} - \mathbf{s}'\|_{\text{EMD}} + 100\mathbb{E}[\xi] = \eta' \cdot \min_{k\text{-sparse } \mathbf{s}'} \|\mathbf{s} - \mathbf{s}'\|_{\text{EMD}} + O\left(\frac{\sqrt{k}}{\lambda\varepsilon}\right)$. Finally, applying Lemma 2.1 concludes the proof. \square

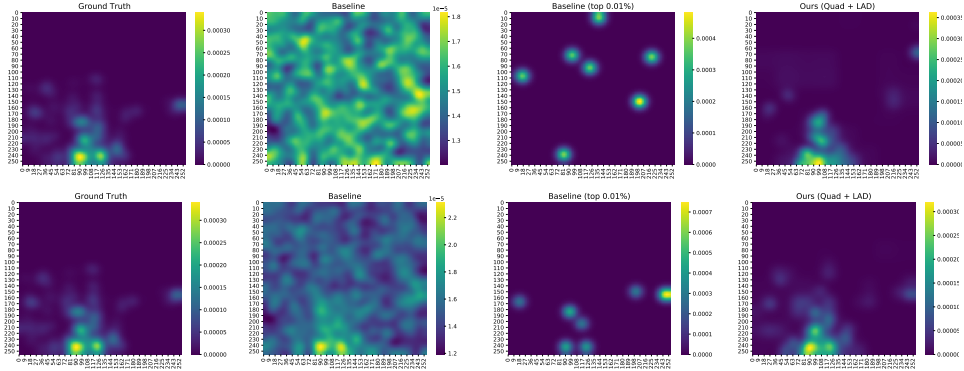


Figure 3: Example visualization of different algorithms for $\varepsilon = 1$ (top) and $\varepsilon = 5$ (bottom). The algorithms from left to right are: original heatmap (no privacy), baseline, baseline with top 0.01% and our algorithm.

4 Experiments

In this section, we study the performance of our algorithms on real-world datasets. Additional experiments on other datasets, including the Salicon image saliency dataset [JHDZ15] and a synthetic dataset, can be found in Appendix E.

Implementation Details. We implement Algorithm 1 with a minor modification: we do not measure at the level $i < q = \lfloor \log \sqrt{w} \rfloor$. In other words, we start directly at the lowest level for which the number of grid cells is at most \sqrt{w} . It is possible to adjust the proof to show that, even with this modification, the error remains $O_\varepsilon(\sqrt{k})$. Apart from this, the algorithm is exactly the same as presented earlier. We note that the linear program at the end of Algorithm 2 can be formulated so that the number of variables is only $O(w\ell)$; the reason is that we only need one variable per cell that is left out at each stage. This allows us to solve it efficiently even when the resolution $\Delta = 2^\ell$ is large.

As for our parameters, we use the decay rate $\gamma = 1/\sqrt{2}$, which is obtained from minimizing the second error term in the proof of Theorem 3.1 as $\ell \rightarrow \infty$ ⁵. We use $w = 20$ in our experiments, which turns out to work well already for datasets we consider. We refrain from tuning parameters further since a privacy analysis of the tuning step has to be taken into account if we want to be completely rigorous. (See, e.g., [LT19] for a formal treatment.)

Datasets. We use two datasets available at snap.stanford.edu to generate the input distribution for users. The first dataset⁶, called GOWALLA, consists of location check-ins by users of the location-based social network Gowalla. Each record consists of, among other things, an anonymized user id together with the latitude (lat) and longitude (lon) of the check-in and a timestamp. We filtered this dataset to consider only check-ins roughly in the continental US (i.e., $\text{lon} \in (-135, -60)$ and $\text{lat} \in (0, 50)$) for the month of January 2010; this resulted in 196,071 check-ins corresponding to 10,196 users. The second dataset⁷, called BRIGHTKITE, also contains check-ins from a different and now defunct location-based social network Brightkite; each record is similar to GOWALLA. Once again, we filtered this dataset to consider only check-ins in the continental US for the months of November and December 2008; this resulted in 304,608 check-ins corresponding to 10,177 users.

For each of these datasets, we partition the whole area into a 300×300 grid. We then took the top 30 cells (in both datasets combined) that have the most check-ins. (Each of the 30 cells is mostly around some city like New York, Austin, etc, and has check-ins from at least 200 unique users). We then consider each cell, partition into $\Delta \times \Delta$ subgrids and snap each check-in to one of these subgrids.

Metrics. To evaluate the quality of an output heatmap $\hat{\mathbf{h}}$ compared to the true heatmap \mathbf{h} , we use the following commonly used metrics: Similarity, Pearson coefficient, KL-divergence, and EMD. (See, e.g., [BJO⁺19] for detailed discussions of these metrics.) We note that the first two metrics should *increase* as $\hat{\mathbf{h}}, \mathbf{h}$ are more similar, whereas the latter two should *decrease*.

Baselines. We consider as a baseline an algorithm recently proposed in [LXD⁺19],⁸ where we simply add Laplace noise to each subgrid cell of the sum \mathbf{s} , zero out any negative cells, and produce the heatmap from this noisy aggregate. We also consider a “thresholding” variant of this baseline that is more suited to sparse data: only keep top $t\%$ of the cell values after noising (and zero out the rest).

4.1 Results

In the first set of experiments, we fix $\Delta = 256$. For each $\varepsilon \in \{0.1, 0.5, 1, 2, 5, 10\}$, we run our algorithms together with the baseline and its variants on all 30 cells, with 2 trials for each cell. In each trial, we sample a set of 200 users and run all the algorithms; we then compute the distance metrics between the true heatmap and the estimated heatmap. The average of these metrics over the 60 runs is presented in Figure 1, together with the 95% confidence interval. As can be seen in the figure, the baseline has rather poor performance across all metrics, even for large $\varepsilon = 10$. We experiment with several values of t for the thresholding variant, which yields a significant improvement. Despite this, we still observe an advantage of our algorithm

⁵When w (and thus q) is fixed, the second error term is proportional to $Z \cdot \sum_{i=0}^{\ell-q-1} \frac{1}{(2\gamma)^i}$ which converges to $\frac{1}{(1-\gamma)(1-0.5/\gamma)}$ as $\ell \rightarrow \infty$. The latter term is minimized when $\gamma = 1/\sqrt{2}$

⁶Available at <http://snap.stanford.edu/data/loc-Gowalla.html>

⁷Available at <http://snap.stanford.edu/data/loc-Brightkite.html>

⁸We remark that [LXD⁺19] also propose using the Gaussian mechanism. However, this algorithm does *not* satisfy ε -DP. Moreover, even when considering (ε, δ) -DP for moderate value of δ (e.g., $\delta = 10^{-3}$), the Gaussian mechanism will still add more noise in expectation than the Laplace mechanism.

consistently across all metrics. These improvements are especially significant when ε is not too large or too small (i.e., $0.2 \leq \varepsilon \leq 5$).

In the second set of experiments, we study the effect of varying the number n of users. By fixing a single cell (with > 500 users) and ε , we sweep $n \in \{50, 100, 200, 300, 400, 500\}$ users. For each value of n , we run 10 trials and average their results. As predicted by theory, our algorithms and the original baseline perform better as n increases. However, the behavior of the thresholding variants of the baseline are less predictable, and sometimes the performance degrades with a larger number of users. It seems plausible that a larger number of users cause an increase in the sparsity, which after some point makes the simple thresholding approach unsuited for the data.

We also run another set of experiments where we fix a single cell and ε , and vary the resolution $\Delta \in \{64, 128, 256\}$. In agreement with theory, our algorithm’s utility remains nearly constant for the entire range of Δ . On the other hand, the original baseline suffers across all metrics as Δ increases. The thresholding variants are more subtle; they occasionally improve as Δ increases, which might be attributed to the fact that when Δ is small, thresholding can zero out too many subgrid cells.

Figure 2 presents results from the latter two set of experiments under the EMD metric when $\varepsilon = 10$. We also include examples of the heatmaps from each approach in Figure 3.

5 Discussions and Future Directions

We present an algorithm for sparse distribution aggregation under the EMD metric, which in turn yields an algorithm for producing heatmaps. As discussed earlier, our algorithm extends naturally to distributed models that can implement the Laplace mechanism, including the secure aggregation model and the shuffle model [BBGN20, GMPV20]. Unfortunately, this does not apply to the more stringent *local* DP model [KLN⁺08] and it remains an interesting open question to devise practical local DP heatmap/EMD aggregation algorithms for “moderate” number of users and privacy parameters.

References

- [Abo18] John M Abowd. The US Census Bureau adopts differential privacy. In *KDD*, pages 2867–2867, 2018.
- [App17] Apple Differential Privacy Team. Learning with privacy at scale. *Apple Machine Learning Journal*, 2017.
- [BBGN20] Borja Balle, James Bell, Adrià Gascón, and Kobbi Nissim. Private summation in the multi-message shuffle model. In *CCS*, pages 657–676, 2020.
- [BDL⁺17] Maria-Florina Balcan, Travis Dick, Yingyu Liang, Wenlong Mou, and Hongyang Zhang. Differentially private clustering in high-dimensional Euclidean spaces. In *ICML*, pages 322–331, 2017.
- [BDMN05] Avrim Blum, Cynthia Dwork, Frank McSherry, and Kobbi Nissim. Practical privacy: the SuLQ framework. In *PODS*, pages 128–138, 2005.
- [BEM⁺17] Andrea Bittau, Úlfar Erlingsson, Petros Maniatis, Ilya Mironov, Ananth Raghunathan, David Lie, Mitch Rudominer, Ushasree Kode, Julien Tinnés, and Bernhard Seefeld. Prochlo: Strong privacy for analytics in the crowd. In *SOSP*, pages 441–459, 2017.

- [BGI⁺08] Radu Berinde, Anna C Gilbert, Piotr Indyk, Howard Karloff, and Martin J Strauss. Combining geometry and combinatorics: A unified approach to sparse signal recovery. In *Allerton*, pages 798–805, 2008.
- [BI09] Radu Berinde and Piotr Indyk. Sequential sparse matching pursuit. In *Allerton*, pages 36–43, 2009.
- [BIR08] Radu Berinde, Piotr Indyk, and Milan Ruzic. Practical near-optimal sparse recovery in the ℓ_1 norm. In *Allerton*, pages 198–205, 2008.
- [BIRW16] Arturs Backurs, Piotr Indyk, Ilya P. Razenshteyn, and David P. Woodruff. Nearly-optimal bounds for sparse recovery in generic norms, with applications to k -median sketching. In *SODA*, pages 318–337, 2016.
- [BJO⁺19] Zoya Bylinskii, Tilke Judd, Aude Oliva, Antonio Torralba, and Frédo Durand. What do different evaluation metrics tell us about saliency models? *PAMI*, 41(3):740–757, 2019.
- [BKM⁺22] Eugene Bagdasaryan, Peter Kairouz, Stefan Mellem, Adrià Gascón, Kallista Bonawitz, Deborah Estrin, and Marco Gruteser. Towards sparse federated analytics: Location heatmaps under distributed differential privacy with secure aggregation. *PoPETS*, 4:162–182, 2022.
- [CGKM21] Alisa Chang, Badih Ghazi, Ravi Kumar, and Pasin Manurangsi. Locally private k -means in one round. In *ICML*, 2021.
- [Cha02] Moses Charikar. Similarity estimation techniques from rounding algorithms. In *STOC*, pages 380–388, 2002.
- [CKS20] Clément L. Canonne, Gautam Kamath, and Thomas Steinke. The discrete Gaussian for differential privacy. In *NeurIPS*, 2020.
- [CNX21] Anamay Chaturvedi, Huy Nguyen, and Eric Xu. Differentially private k -means clustering via exponential mechanism and max cover. *AAAI*, 2021.
- [CPS⁺12] Graham Cormode, Cecilia M. Procopiuc, Divesh Srivastava, Entong Shen, and Ting Yu. Differentially private spatial decompositions. In *ICDE*, pages 20–31, 2012.
- [CPST12] Graham Cormode, Cecilia Procopic, Divesh Srivastava, and Thanh T. L. Tran. Differentially private summaries for sparse data. In *ICDT*, pages 299–311, 2012.
- [CSU⁺19] Albert Cheu, Adam D. Smith, Jonathan Ullman, David Zeber, and Maxim Zhilyaev. Distributed differential privacy via shuffling. In *EUROCRYPT*, pages 375–403, 2019.
- [DKM⁺06] Cynthia Dwork, Krishnaram Kenthapadi, Frank McSherry, Ilya Mironov, and Moni Naor. Our data, ourselves: Privacy via distributed noise generation. In *EUROCRYPT*, pages 486–503, 2006.
- [DKY17] Bolin Ding, Janardhan Kulkarni, and Sergey Yekhanin. Collecting telemetry data privately. In *NeurIPS*, pages 3571–3580, 2017.
- [DMNS06] Cynthia Dwork, Frank McSherry, Kobbi Nissim, and Adam Smith. Calibrating noise to sensitivity in private data analysis. In *TCC*, pages 265–284, 2006.

- [DSS⁺15] Cynthia Dwork, Adam D. Smith, Thomas Steinke, Jonathan R. Ullman, and Salil P. Vadhan. Robust traceability from trace amounts. In Venkatesan Guruswami, editor, *FOCS*, pages 650–669, 2015.
- [EFM⁺19] Úlfar Erlingsson, Vitaly Feldman, Ilya Mironov, Ananth Raghunathan, Kunal Talwar, and Abhradeep Thakurta. Amplification by shuffling: From local to central differential privacy via anonymity. In *SODA*, pages 2468–2479, 2019.
- [EPK14] Úlfar Erlingsson, Vasyl Pihur, and Aleksandra Korolova. RAPPOR: Randomized aggregatable privacy-preserving ordinal response. In *CCS*, pages 1054–1067, 2014.
- [FFKN09] Dan Feldman, Amos Fiat, Haim Kaplan, and Kobbi Nissim. Private coresets. In *STOC*, pages 361–370, 2009.
- [FXZR17] Dan Feldman, Chongyuan Xiang, Ruihao Zhu, and Daniela Rus. Coresets for differentially private k -means clustering and applications to privacy in mobile sensor networks. In *IPSN*, pages 3–16, 2017.
- [GD04] K. Grauman and T. Darrell. Fast contour matching using approximate earth mover’s distance. In *CVPR*, pages 220–227, 2004.
- [GKM20] Badih Ghazi, Ravi Kumar, and Pasin Manurangsi. Differentially private clustering: Tight approximation ratios. In *NeurIPS*, 2020.
- [GLM⁺10] Anupam Gupta, Katrina Ligett, Frank McSherry, Aaron Roth, and Kunal Talwar. Differentially private combinatorial optimization. In *SODA*, pages 1106–1125, 2010.
- [GMPV20] Badih Ghazi, Pasin Manurangsi, Rasmus Pagh, and Ameya Velingker. Private aggregation from fewer anonymous messages. In *EUROCRYPT*, pages 798–827, 2020.
- [Gre16] Andy Greenberg. Apple’s “differential privacy” is about collecting your data – but not your data. *Wired*, June, 13, 2016.
- [HL18] Zhiyi Huang and Jinyan Liu. Optimal differentially private algorithms for k -means clustering. In *PODS*, pages 395–408, 2018.
- [HM04] Sariel Har-Peled and Soham Mazumdar. On coresets for k -means and k -median clustering. In *STOC*, pages 291–300, 2004.
- [HT10] Moritz Hardt and Kunal Talwar. On the geometry of differential privacy. In *STOC*, pages 705–714, 2010.
- [IBC⁺12] Sibren Isaacman, Richard Becker, Ramón Cáceres, Margaret Martonosi, James Rowland, Alexander Varshavsky, and Walter Willinger. Human mobility modeling at metropolitan scales. In *MobiSys*, pages 239–252, 2012.
- [IP11] Piotr Indyk and Eric Price. k -median clustering, model-based compressive sensing, and sparse recovery for earth mover distance. In *STOC*, pages 627–636, 2011.
- [IR08] Piotr Indyk and Milan Ruzic. Near-optimal sparse recovery in the L1 norm. In *FOCS*, pages 199–207, 2008.
- [IT03] Piotr Indyk and Nitin Thaper. Fast color image retrieval via embeddings. In *Workshop on Statistical and Computational Theories of Vision (at ICCV)*, 2003, 2003.

- [JHDZ15] Ming Jiang, Shengsheng Huang, Juanyong Duan, and Qi Zhao. Salicon: Saliency in context. In *CVPR*, 2015.
- [JNN21] Matthew Jones, Huy Le Nguyen, and Thy Nguyen. Differentially private clustering via maximum coverage. In *AAAI*, 2021.
- [KLN⁺08] Shiva Prasad Kasiviswanathan, Homin K. Lee, Kobbi Nissim, Sofya Rashkodnikova, and Adam Smith. What can we learn privately? In *FOCS*, pages 531–540, 2008.
- [KSS17] Bart Kranstauber, Marco Smolla, and Kamran Safi. Similarity in spatial utilization distributions measured by the earth mover’s distance. *Methods in Ecology and Evolution*, 8(2):155–160, 2017.
- [LB01] Elizaveta Levina and Peter Bickel. The earth mover’s distance is the Mallows distance: Some insights from statistics. In *ICCV*, pages 251–256, 2001.
- [LT19] Jingcheng Liu and Kunal Talwar. Private selection from private candidates. In Moses Charikar and Edith Cohen, editors, *STOC*, pages 298–309, 2019.
- [LXD⁺19] Ao Liu, Lirong Xia, Andrew Duchowski, Reynold Bailey, Kenneth Holmqvist, and Eakta Jain. Differential privacy for eye-tracking data. In *ETRA*, pages 1–10, 2019.
- [MTS⁺12] Prashanth Mohan, Abhradeep Thakurta, Elaine Shi, Dawn Song, and David Culler. GUPT: privacy preserving data analysis made easy. In *SIGMOD*, pages 349–360, 2012.
- [NCBN16] Richard Nock, Raphaël Canyasse, Roksana Boreli, and Frank Nielsen. k -variates++: more pluses in the k -means++. In *ICML*, pages 145–154, 2016.
- [NRS07] Kobbi Nissim, Sofya Raskhodnikova, and Adam Smith. Smooth sensitivity and sampling in private data analysis. In *STOC*, pages 75–84, 2007.
- [NS18] Kobbi Nissim and Uri Stemmer. Clustering algorithms for the centralized and local models. In *ALT*, pages 619–653, 2018.
- [NSV16] Kobbi Nissim, Uri Stemmer, and Salil P. Vadhan. Locating a small cluster privately. In *PODS*, pages 413–427, 2016.
- [PRTB99] J. Puzicha, Y. Rubner, C. Tomasi, and J. M. Buhmann. Empirical evaluation of dissimilarity measures for color and texture. In *ICCV*, pages 1165–1173, 1999.
- [QYL13] Wahbeh H. Qardaji, Weining Yang, and Ninghui Li. Understanding hierarchical methods for differentially private histograms. *VLDB*, 6(14):1954–1965, 2013.
- [RE19] Carey Radebaugh and Ulfar Erlingsson. Introducing TensorFlow Privacy: Learning with Differential Privacy for Training Data, March 2019. blog.tensorflow.org.
- [RTG98] Y. Rubner, C. Tomasi, and L.J. Guibas. A metric for distributions with applications to image databases. In *ICCV*, pages 59–66, 1998.
- [RTG00] Yossi Rubner, Carlo Tomasi, and Leonidas J Guibas. The earth mover’s distance as a metric for image retrieval. *IJCV*, 40(2):99–121, 2000.
- [SCL⁺16] Dong Su, Jianneng Cao, Ninghui Li, Elisa Bertino, and Hongxia Jin. Differentially private k -means clustering. In *CODASPY*, pages 26–37, 2016.

- [Sha14] Stephen Shankland. How Google tricks itself to protect Chrome user privacy. *CNET*, October, 2014.
- [SHHB19] Julian Steil, Inken Hagestedt, Michael Xuelin Huang, and Andreas Bulling. Privacy-aware eye tracking using differential privacy. In *ETRA*, pages 1–9, 2019.
- [SK18] Uri Stemmer and Haim Kaplan. Differentially private k -means with constant multiplicative error. In *NeurIPS*, pages 5436–5446, 2018.
- [SO95] M. Stricker and M. Orengo. Similarity of color images. In *SPIE*, pages 381–392, 1995.
- [Ste20] Uri Stemmer. Locally private k -means clustering. In *SODA*, pages 548–559, 2020.
- [TM20] Davide Testuggine and Ilya Mironov. PyTorch Differential Privacy Series Part 1: DP-SGD Algorithm Explained, August 2020. medium.com.
- [WG12] Fan Wang and Leonidas J Guibas. Supervised earth mover’s distance learning and its computer vision applications. In *ECCV*, pages 442–455, 2012.
- [WWS15] Yining Wang, Yu-Xiang Wang, and Aarti Singh. Differentially private subspace clustering. In *NeurIPS*, pages 1000–1008, 2015.
- [XYL08] D. Xu, S. Yan, and J. Luo. Face recognition using spatially constrained earth mover’s distance. *Trans. Image Processing*, 17(11):2256–2260, 2008.
- [ZXX16] Jun Zhang, Xiaokui Xiao, and Xing Xie. Privtree: A differentially private algorithm for hierarchical decompositions. In *SIGMOD*, pages 155–170, 2016.
- [ZYT08] Q. Zhao, Z. Yang, and H. Tao. Differential earth mover’s distance with its applications to visual tracking. *PAMI*, 32:274–287, 2008.

A Implications for Planar k -Median

Sparse EMD aggregation is intimately related to clustering, specifically, the planar k -median problem. Indeed, as already noted (somewhat implicitly) by [IP11, BIRW16], an algorithm for sparse EMD aggregation immediately implies a coresets [HM04] for k -median on the plane, which in turn can be used to derive an approximation algorithm for the problem.

Before we can state our results, recall that in the *planar k -median* problem, each user has a point $x_i \in [0, 1]^2$. The goal is to output a set $C \subseteq [0, 1]^2$ of k centers that minimizes the following objective:

$$\text{cost}_C(X) := \sum_{x \in X} \min_{c \in C} \|c - x\|_1,$$

where $X = (x_1, \dots, x_n)$.

The above cost notation extends naturally to that of a non-negative vector $\mathbf{x} \in \mathbb{R}_{\geq 0}^{G_\Delta}$. More specifically, we can define

$$\text{cost}_C(\mathbf{x}) := \sum_{u \in G_\Delta} \mathbf{x}(u) \cdot \min_{c \in C} \|c - u\|_1.$$

Definition A.1 (Coreset). Let $\lambda \in (0, 1)$ and $\kappa > 0$. \mathbf{x} is said to be a (λ, κ) -coreset for X (with respect to k -median objective) iff, for every $C \subseteq [0, 1]^2$ of size k , we have $(1 - \lambda) \cdot \text{cost}_C(X) - \kappa \leq \text{cost}_C(\mathbf{x}) \leq (1 + \lambda) \cdot \text{cost}_C(X) + \kappa$.

In this context, our results immediately imply the following:

Corollary A.1. *There exists an ε -DP algorithm that, for any constant $\lambda \in (0, 1)$, can output a $(\lambda, O(\sqrt{k}/\varepsilon))$ -coreset for k -median, where each input point belongs to $[0, 1]^2$.*

Corollary A.2. *There exists an ε -DP algorithm that, for any constant $\lambda \in (0, 1)$, can output a $(1 + \lambda, O(\sqrt{k}/\varepsilon))$ -approximation for k -median, where each input point belongs to $[0, 1]^2$.*

There have been numerous works studying DP clustering algorithms [BDMN05, NRS07, FFKN09, GLM⁺10, MTS⁺12, WWS15, NSV16, NCBN16, SCL⁺16, FXZR17, BDL⁺17, NS18, HL18, NCBN16, NS18, SK18, Ste20, GKM20, JNN21, CNX21, CGKM21], each with varying guarantees. Many of these works either considered the low-dimensional case directly (e.g., [FFKN09]), or used it as a subroutine (e.g., [BDL⁺17, GKM20]). Despite this, each of these works incurs an additive error of $\Omega(k)$, while our results above achieve an improved $O(\sqrt{k})$ additive error; this bound is also tight due to a simple adaptation of our lower bound for k -sparse distribution aggregation. Another surprising aspect of our guarantee is that the additive error is *independent* of the number n of users. To the best of our knowledge, all previous results incur an additive error that depends on n .

We will now prove Corollary A.1 and Corollary A.2. In both cases, we will assume that each point (together with the centers) belongs to G_Δ , where $\Delta = \lceil \log(\varepsilon/(n\sqrt{k})) \rceil$. Indeed, if a point was not from G_Δ , then we can simply replace it with the closest point in G_Δ , which would introduce an additive error of at most $O(\sqrt{k}/\varepsilon)$.

Below we use the notation, $\mathbf{1}_S$ to denote the indicator vector of S , i.e.,

$$\mathbf{1}_S(a) = \begin{cases} 1 & \text{if } a \in S, \\ 0 & \text{otherwise.} \end{cases}$$

Proof of Corollary A.1. We view the input point x_i as the indicator vector $\mathbf{p}_i = \mathbf{1}_{x_i}$. We then run Algorithm 1 but output $\mathbf{x} = \hat{\mathbf{s}}$ (instead of the normalized $\hat{\mathbf{s}}/\|\hat{\mathbf{s}}\|_{\text{EMD}}$). Recall from the proof of Theorem 3.1 that, with appropriate setting of parameters, the output satisfies

$$\|\mathbf{s} - \hat{\mathbf{s}}\|_{\text{EMD}} \leq \lambda \cdot \min_{k\text{-sparses}'} \|\mathbf{s} - \mathbf{s}'\|_{\text{EMD}} + O(\sqrt{k}/\varepsilon), \quad (5)$$

where \mathbf{s} represents $\sum_{i \in [n]} \mathbf{p}_i$.

Consider any set C of at most k centers. We have

$$\begin{aligned} & |\text{cost}_C(X) - \text{cost}_C(\mathbf{x})| \\ & \leq \|\mathbf{s} - \hat{\mathbf{s}}\|_{\text{EMD}} \\ & \stackrel{(5)}{\leq} \lambda \cdot \min_{k\text{-sparses}'} \|\mathbf{s} - \mathbf{s}'\|_{\text{EMD}} + O(\sqrt{k}/\varepsilon) \\ & \leq \lambda \cdot \text{cost}_C(X) + O(\sqrt{k}/\varepsilon), \end{aligned}$$

which concludes our proof. □

Corollary A.2 then follows from Corollary A.1 by simply running any non-private algorithm for k -median on top of the coreset produced by Corollary A.1.

B Relationship between Heatmaps Aggregation and EMD Aggregation

Aggregating distributions under EMD is closely related to aggregating heatmaps. In this section we formalize this relationship by showing that EMD bound on the error of the distribution aggregation problem yields many types of error bounds of aggregating a slight variant of heatmaps, which we call “infinite” heatmaps. The latter is the same as the usual heatmaps except that we do not truncate the distribution around the border. More specifically, we let $\tilde{G}_\Delta := \{(i/\Delta, j/\Delta) \mid i, j \in \mathbb{Z}\}$ and

$$\tilde{H}_\mathbf{p}^\sigma(a) = \sum_{a' \in G_\Delta} \frac{1}{Z} e^{-\frac{\|a-a'\|_2^2}{2\sigma^2}} \cdot p(a'),$$

for all $a \in \tilde{G}_\Delta$, where $Z := \sum_{d \in \tilde{G}_\Delta} e^{-\frac{\|d\|_2^2}{2\sigma^2}}$ is the normalization factor.

We conjecture that (slight variants of) the bounds we discuss below also hold for the standard (truncated) version of heatmaps.

Bound on EMD. We start with the simplest bound: that of EMD on the (infinite) heatmaps.

Lemma B.1. For any $\mathbf{p}, \mathbf{q} \in \mathbb{R}_{\geq 0}^{G_\Delta}$ such that $\|\mathbf{p}\|_1 = \|\mathbf{q}\|_1$ and $\sigma > 0$, we have

$$\text{EMD}(\tilde{H}_\mathbf{p}^\sigma, \tilde{H}_\mathbf{q}^\sigma) \leq \text{EMD}(\mathbf{p}, \mathbf{q}).$$

Proof. Let γ be such that

$$\text{EMD}(\mathbf{p}, \mathbf{q}) = \sum_{a \in G_\Delta} \sum_{b \in G_\Delta} \gamma(a, b) \cdot \|a - b\|_1,$$

and γ 's marginals are equal to \mathbf{p}, \mathbf{q} . For convenience, we let $\gamma(a, b)$ be zero when $a \notin G_\Delta$ or $b \notin G_\Delta$. We then define $\tilde{\gamma}$ on $\tilde{G}_\Delta \times \tilde{G}_\Delta$ by

$$\tilde{\gamma}(a, b) = \sum_{d \in \tilde{G}_\Delta} \frac{1}{Z} \cdot e^{-\frac{\|d\|_2^2}{2\sigma^2}} \cdot \gamma(a + d, b + d).$$

It is simple to check that the marginals of $\tilde{\gamma}$ are exactly $\tilde{H}_\mathbf{p}^\sigma, \tilde{H}_\mathbf{q}^\sigma$. As such, we have

$$\begin{aligned} & \text{EMD}(\tilde{H}_\mathbf{p}^\sigma, \tilde{H}_\mathbf{q}^\sigma) \\ & \leq \sum_{a \in \tilde{G}_\Delta} \sum_{b \in \tilde{G}_\Delta} \tilde{\gamma}(a, b) \cdot \|a - b\|_1 \\ & = \sum_{a \in \tilde{G}_\Delta} \sum_{b \in \tilde{G}_\Delta} \|a - b\|_1 \cdot \left(\sum_{d \in \tilde{G}_\Delta} \frac{1}{Z} \cdot e^{-\frac{\|d\|_2^2}{2\sigma^2}} \cdot \gamma(a + d, b + d) \right) \\ & = \sum_{a', b' \in \tilde{G}_\Delta} \gamma(a', b') \cdot \|a' - b'\|_1 \cdot \left(\sum_{d \in \tilde{G}_\Delta} \frac{1}{Z} \cdot e^{-\frac{\|d\|_2^2}{2\sigma^2}} \right) \\ & = \text{EMD}(\mathbf{p}, \mathbf{q}). \end{aligned}$$

where the penultimate equality is from substituting $a' = a + d$ and $b' = b + d$. □

Bound on KL-divergence. We will now move on to the KL-divergence. For this purpose, we will use the following bound, shown in [CKS20]⁹. Here we use $\mathbf{1}_p$ to denote the indicator variable for the point p , i.e., a vector that is equal to one at coordinate p and zero elsewhere.

Lemma B.2 ([CKS20, Proposition 5]). *For any $a, b \in G_\Delta$ and $\sigma > 0$, we have*

$$\text{KL}(\tilde{H}_{\mathbf{1}_a}^\sigma \| \tilde{H}_{\mathbf{1}_b}^\sigma) \leq \frac{\|a - b\|_2^2}{2\sigma^2}.$$

We can now prove that EMD on the distribution aggregation error implies a KL-divergence bound of the (infinite) heatmaps:

Lemma B.3. *For any $\mathbf{p}, \mathbf{q} \in \mathbb{R}_{\geq 0}^{G_\Delta}$ such that $\|\mathbf{p}\|_1 = \|\mathbf{q}\|_1 = 1$ and $\sigma > 0$, we have*

$$\text{KL}(\tilde{H}_{\mathbf{p}}^\sigma \| \tilde{H}_{\mathbf{q}}^\sigma) \leq \frac{\text{EMD}(\mathbf{p}, \mathbf{q})}{2\sigma^2}.$$

Proof. Let γ be such that

$$\text{EMD}(\mathbf{p}, \mathbf{q}) = \sum_{a \in G_\Delta} \sum_{b \in G_\Delta} \gamma(a, b) \cdot \|a - b\|_1,$$

and γ 's marginals are equal to \mathbf{p}, \mathbf{q} .

From the convexity of KL-divergence, we have

$$\begin{aligned} \text{KL}(\tilde{H}_{\mathbf{p}}^\sigma, \tilde{H}_{\mathbf{q}}^\sigma) &\leq \sum_{a \in G_\Delta} \sum_{b \in G_\Delta} \gamma(a, b) \cdot \text{KL}(\tilde{H}_{\mathbf{1}_a}^\sigma, \tilde{H}_{\mathbf{1}_b}^\sigma) \\ &\stackrel{\text{(Lemma B.2)}}{\leq} \sum_{a \in G_\Delta} \sum_{b \in G_\Delta} \gamma(a, b) \cdot \frac{\|a - b\|_2^2}{2\sigma^2} \\ &\stackrel{\text{(From } a, b \in [0, 1])}{\leq} \sum_{a \in G_\Delta} \sum_{b \in G_\Delta} \gamma(a, b) \cdot \frac{\|a - b\|_1}{2\sigma^2} \\ &\leq \frac{\text{EMD}(\mathbf{p}, \mathbf{q})}{2\sigma^2}. \quad \square \end{aligned}$$

Bound on TV distance and Similarity. Via Pinsker's inequality and our previous bound on the KL-divergence, we arrive at the following:

Lemma B.4. *For any $\mathbf{p}, \mathbf{q} \in \mathbb{R}_{\geq 0}^{G_\Delta}$ such that $\|\mathbf{p}\|_1 = \|\mathbf{q}\|_1 = 1$ and $\sigma > 0$, we have*

$$\text{TV}(\tilde{H}_{\mathbf{p}}^\sigma \| \tilde{H}_{\mathbf{q}}^\sigma) \leq \frac{\sqrt{\text{EMD}(\mathbf{p}, \mathbf{q})}}{2\sigma}.$$

Finally, recall that the similarity (SIM) metric is simply one minus the total variation distance; this, together with the above lemma, leads to the following bound:

Corollary B.5. *For any $\mathbf{p}, \mathbf{q} \in \mathbb{R}_{\geq 0}^{G_\Delta}$ such that $\|\mathbf{p}\|_1 = \|\mathbf{q}\|_1 = 1$ and $\sigma > 0$, we have*

$$\text{SIM}(\tilde{H}_{\mathbf{p}}^\sigma \| \tilde{H}_{\mathbf{q}}^\sigma) \geq 1 - \frac{\sqrt{\text{EMD}(\mathbf{p}, \mathbf{q})}}{2\sigma}.$$

⁹Strictly speaking, [CKS20] only states the lemma for the 1-dimensional case but it is not hard to see that it holds for the 2-dimensional case of our interest as well.

C A Tight Lower Bound for Sparse EMD Aggregation

Our lower bounds in this and the subsequent section apply for any sufficiently large Δ (depending on the other parameters); this will be assumed without explicitly stated in the subsequent statement of the theorems/lemmas. We remark that this is necessary because if Δ is too small, then one can get smaller error. (E.g., if $\Delta = 1$, it is obvious how to get $O(1/\varepsilon)$ error.)

The main result of this section is a lower bound of $\Omega_\varepsilon(\sqrt{k}/n)$ on the additive error of any ε -DP algorithm for sparse EMD aggregation, which matches the error bounds we achieved in our algorithm (Theorem 3.1):

Theorem C.1. *For any $\lambda, \varepsilon > 0$, any integers $k \geq \varepsilon$ and $n \geq k/\varepsilon$, no ε -DP algorithm can, on input consisting of n distributions, output a $(\lambda, o(\frac{\sqrt{k}}{\varepsilon n}))$ -approximation for sparse EMD aggregation, with probability at least 0.1.*

We prove the above result via the packing framework of Hardt and Talwar [HT10]. Recall that we say that a set of k -sparse probability distributions $\mathbf{p}_1, \dots, \mathbf{p}_T$ is a γ -packing (for EMD distance) if $\text{EMD}(\mathbf{p}_i, \mathbf{p}_j) \geq \gamma$ for all $i, j \in \{1, \dots, T\}$; the size of the packing is T . The following lemma provides such a packing with large size, based on constructing an ℓ_1 packing on a $\sqrt{k} \times \sqrt{k}$ grid.

Lemma C.2. *For any $\gamma > 0$ such that $\gamma < 0.01/\sqrt{k}$, there exists a set of k -sparse probability distributions that forms a γ -packing of size $2^{\Omega(k \cdot \log(1/(\gamma\sqrt{k})))}$. Furthermore, we can pick the packing so that each of its elements (i.e., distributions) has the same support.*

Proof. Consider the grid points G_t where t is the smallest power of two that is no larger than \sqrt{k} . Let \mathcal{H} denote any maximal subset of $S := \{\mathbf{r} \in \mathbb{R}_{\geq 0}^d \mid \|\mathbf{r}\|_1 = 0.5\}$ such that the pairwise ℓ_1 distance of elements of \mathcal{H} is at least $2\gamma t$. (In other words, \mathcal{H} is a $(2\gamma t)$ -packing of S under ℓ_1 distance.) Due to the maximality of \mathcal{H} , the ℓ_1 balls of radius $2\gamma t$ around elements of \mathcal{H} must cover S . Recall that the volume of d -dimensional ℓ_1 ball of radius r is $(2r)^d/d!$. Thus, we have

$$|\mathcal{H}| \geq \frac{\text{Vol}(S)}{(4\gamma t)^d/d!} = \frac{0.5^d/d!}{(4\gamma t)^d/d!} \geq 2^{\Omega(k \cdot \log(1/(\gamma\sqrt{k})))},$$

where in the equality we use the fact that the d -simplex has volume $1/d!$ and in the second inequality we use the fact that $t = \Theta(\sqrt{k})$ and $d = t^2 = \Theta(k)$.

Finally, we create our packing \mathcal{P} as follows: for every $\mathbf{r} \in \mathcal{H}$, add to \mathcal{P} the distribution \mathbf{p} defined by $\mathbf{p}(a) = \mathbf{r}(a) + 0.5/t^2$ for all $a \in G_t$. Now, notice that, for any pair of distributions \mathbf{p}, \mathbf{q} over G_t , we have $\text{EMD}(\mathbf{p}, \mathbf{q}) \geq \|\mathbf{p} - \mathbf{q}\|/(2t)$ because any two points in G_t are of distance at least $1/t$ apart; thus \mathcal{P} is indeed a γ -packing. Furthermore, since $|G_t| \leq t^2 \leq k$, any probability distribution over G_t is k -sparse as desired. \square

We can now apply the packing framework [HT10] to prove Theorem C.1:

Proof of Theorem C.1. Let $\gamma = \Omega(1/\sqrt{k})$ denote the largest γ for which Lemma C.2 guarantees the existence of γ -packing $\mathcal{P} = \{\mathbf{p}_1, \dots, \mathbf{p}_T\}$ of size (at least) $10 \cdot e^k$. Let $n_0 := \lfloor k/\varepsilon \rfloor$, and consider any $n \geq n_0$.

Suppose for the sake of contradiction that there is an ε -DP algorithm \mathbb{A} that with probability at least 0.1 outputs an $(\lambda, 0.4\gamma n_0/n)$ -approximation. (Note that, since $k \geq \varepsilon$, $0.4\gamma n_0/n = \Omega(\frac{\sqrt{k}}{\varepsilon n})$.) Let \mathbf{p}^* be any element of \mathcal{P} . For every distinct $\mathbf{p} \in \mathcal{P}$, let $B_{\mathbf{p}}$ denote the set of all \mathbf{q} such that $\text{EMD}(\mathbf{q}, \frac{n_0}{n} \cdot \mathbf{p} + \frac{n-n_0}{n} \cdot \mathbf{p}^*) \leq 0.4\gamma$. Furthermore, let $\mathbf{X}_{\mathbf{p}}$ denote the dataset consisting of n_0 copies of \mathbf{p} and $n - n_0$ copies of \mathbf{p}^* . Note

that the average distribution of $\mathbf{X}_{\mathbf{p}}$ is k -sparse, since every distribution in \mathcal{P} is k -sparse and has the same support. Hence, from the assumed accuracy guarantee of \mathbb{A} , we have

$$\Pr[\mathbb{A}(\mathbf{X}_{\mathbf{p}}) \in B_{\mathbf{p}}] \geq 0.1.$$

Next, let \mathbf{X}^* denote the dataset consisting of $n - n_0$ copies of \mathbf{p}^* . From the ε -DP guarantee of \mathbb{A} , we have

$$\Pr[\mathbb{A}(\mathbf{X}^*) \in B_{\mathbf{p}}] \geq e^{-\varepsilon n_0} \cdot \Pr[\mathbb{A}(\mathbf{X}_{\mathbf{p}})] \geq 0.1 \cdot e^{-k}. \quad (6)$$

Now, notice that $B_{\mathbf{p}}$ are disjoint for all $\mathbf{p} \in \mathcal{P}$ because \mathcal{P} forms a γ -packing. Thus, we have

$$\begin{aligned} \Pr \left[\mathbb{A}(\mathbf{X}^*) \in \bigcup_{\mathbf{p} \in \mathcal{P}} B_{\mathbf{p}} \right] &= \sum_{\mathbf{p} \in \mathcal{P}} \Pr [\mathbb{A}(\mathbf{X}^*) \in B_{\mathbf{p}}] \\ &\stackrel{(6)}{\geq} |\mathcal{P}| \cdot 0.1 \cdot e^{-k} > 1, \end{aligned}$$

a contradiction. □

D Dense EMD Aggregation: Tight Bounds

In this section, we consider the distribution aggregation under EMD but without any sparsity constraint. We will show that in this case the tight EMD error is $\tilde{\Theta}(1/\sqrt{\varepsilon n})$. Notice that this is a factor $\tilde{\Theta}_{\varepsilon}(\sqrt{n/k})$ larger than the additive error in our sparse EMD aggregation (Theorem 3.1).

D.1 Algorithm

In this section, we present a simple algorithm for EMD aggregation that yields the claimed bound.

Theorem D.1. *For any $\varepsilon > 0$, there exists an ε -DP algorithm for EMD aggregation that with probability 0.99 incurs an expected error of $\tilde{O}(1/\sqrt{\varepsilon n})$.*

Proof. Let $\ell^* = \log \sqrt{\varepsilon n}$ and let $\Delta^* = 2^{\ell^*}$. Our algorithm starts by snapping every point to the closest point in t ; more formally, we consider user i 's input to be $P_t \mathbf{p}_i$ instead of the original \mathbf{p}_i . This can contribute to at most $\sqrt{\varepsilon n}$ in the additive error, and henceforth we may assume that each input \mathbf{p}_i belongs to $\mathbb{R}_{\geq 0}^{G_{\Delta^*}}$ (i.e., $\Delta = \Delta^*$) instead.

From here, we just compute the sum $\mathbf{s} := \sum_{i=1}^n \mathbf{p}_i$ and add Laplace noise to get $\tilde{\mathbf{s}} = \mathbf{s} + \nu$ where $\nu(a) \sim \text{Lap}(1/\varepsilon)$ for each $a \in G_{\Delta}$. Then, we find $\hat{\mathbf{s}} \in \mathbb{R}_{\geq 0}^{G_t}$ that minimizes $\|\hat{\mathbf{s}} - \tilde{\mathbf{s}}\|_{\text{EMD}}$. (This can be formulated as a linear program.) Finally, output $\hat{\mathbf{a}} = \hat{\mathbf{s}}/\|\hat{\mathbf{s}}\|_1$.

It is straightforward that the algorithm is ε -DP, since it consists of only applying the Laplace mechanism once and post-processing its result. Next, we will analyze its utility. From Lemma 2.1 and Markov's inequality, it suffices to show that $\mathbb{E}[\|\hat{\mathbf{s}} - \mathbf{s}\|_{\text{EMD}}] \leq \tilde{O}(\sqrt{n/\varepsilon})$. Due to the triangle inequality, we have

$$\begin{aligned} \|\hat{\mathbf{s}} - \mathbf{s}\|_{\text{EMD}} &\leq \|\hat{\mathbf{s}} - \tilde{\mathbf{s}}\|_{\text{EMD}} + \|\tilde{\mathbf{s}} - \mathbf{s}\|_{\text{EMD}} \\ &\leq 2 \cdot \|\tilde{\mathbf{s}} - \mathbf{s}\|_{\text{EMD}} = 2\|\nu\|_{\text{EMD}}, \end{aligned}$$

where the latter inequality follows from how $\hat{\mathbf{s}}$ is computed. As a result, it suffices to show that $\mathbb{E}[\|\nu\|_{\text{EMD}}] \leq \tilde{O}(\sqrt{n/\varepsilon})$, which we do next.

From Lemma 3.5, we have

$$\mathbb{E}[\|\nu\|_{\text{EMD}}]$$

$$\begin{aligned}
&\leq \mathbb{E}[\|\mathbf{P}\nu\|_1] \\
&= \sum_{i \in [\ell^*]} 2^{-i} \mathbb{E}[\|\mathbf{P}_i \nu\|_1] \\
&= \sum_{i \in [\ell^*]} 2^{-i} \sum_{c \in C^{2^i}} \mathbb{E} \left[\left\| \sum_{p \in c \cap G_\Delta} \nu(p) \right\| \right]
\end{aligned}$$

by the Cauchy–Schwarz inequality

$$\leq \sum_{i \in [\ell^*]} 2^{-i} \sum_{c \in C^{2^i}} \sqrt{\mathbb{E} \left[\left(\sum_{p \in c \cap G_\Delta} \nu(p) \right)^2 \right]}$$

by the independence of $\nu(i)$

$$\begin{aligned}
&= \sum_{i \in [\ell^*]} 2^{-i} \sum_{c \in C^{2^i}} \sqrt{\mathbb{E} \left[\sum_{p \in c \cap G_\Delta} \nu(p)^2 \right]} \\
&= \sum_{i \in [\ell^*]} 2^{-i} \sum_{c \in C^{2^i}} \sqrt{|p \in c \cap G_\Delta| \cdot \frac{2}{\varepsilon^2}} \\
&\leq O \left(\sum_{i \in [\ell^*]} 2^{-i} \sum_{c \in C^{2^i}} 2^{\ell^* - i} \cdot \frac{1}{\varepsilon} \right) \\
&= O \left(\sum_{i \in [\ell^*]} 2^{-i} \cdot 2^{2i} \cdot 2^{\ell^* - i} \cdot \frac{1}{\varepsilon} \right) \\
&= O \left(\ell^* \cdot 2^{\ell^*} / \varepsilon \right) \\
&= O \left(\log(\varepsilon n) \cdot \sqrt{\varepsilon n} / \varepsilon \right) \\
&= \tilde{O}(\sqrt{n/\varepsilon}). \quad \square
\end{aligned}$$

D.2 Lower Bound

A matching lower bound can be immediately obtain from plugging in $k = \lfloor \varepsilon n \rfloor$ into our lower bound for the sparse case (Theorem C.1). This immediately yields the following.

Corollary D.2. *For any $\varepsilon > 0$ and any integer $n \geq \varepsilon$, no ε -DP algorithm can incur an error at most $o(1/\sqrt{\varepsilon n})$ for EMD aggregation with probability at least 0.1.*

E Additional Experiment Results

E.1 Additional Results on Geo Datasets

Recall the second (varying the number of users) and third (varying the resolution) experimental setups described in Section 4.1. We had presented the results on the EMD metric in Figure 2. Results on other

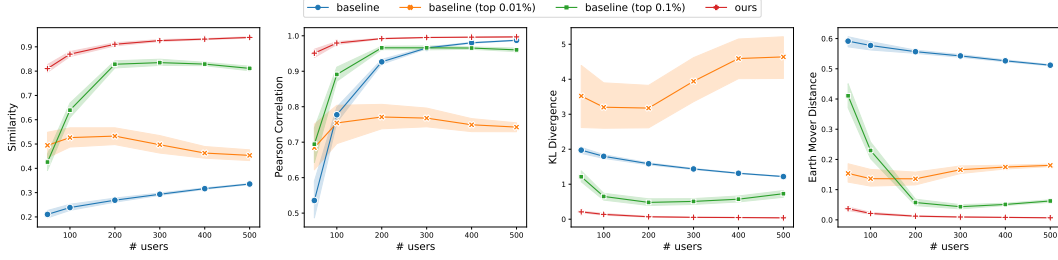


Figure 4: Effect of the # users on different metrics ($\varepsilon = 10$). Shaded areas indicate 95% confidence interval.

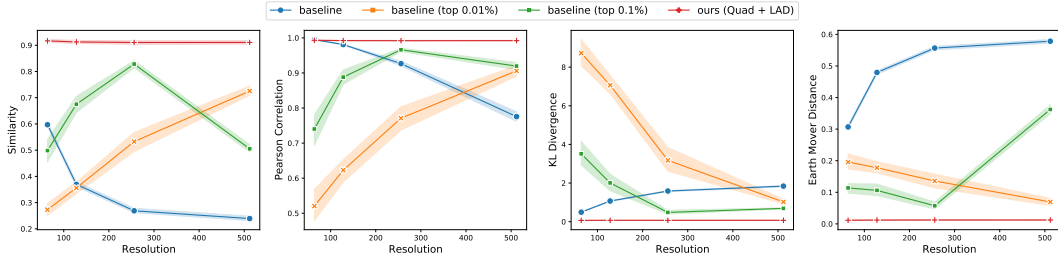


Figure 5: Effect of the resolution on different metrics ($\varepsilon = 10$). Shaded areas indicate 95% confidence interval.

metrics can be found in Figure 4 and Figure 5, respectively. Other parameters are fixed as before, e.g., $\varepsilon = 10$. The trends are similar across all metrics.

As predicted by theory, the utility of both the baseline and our algorithm increases with n , the number of users. On the other hand, the threshold variants of the baseline initially performs better as n increases but after some point it starts to become worse. A possible reason is that, as n increases, the sparsity level (i.e., the number of non-zero cells after aggregation) also increases, and thus thresholding eventually becomes too aggressive and loses too much information.

In terms of the resolution Δ , our algorithm's utility remains nearly constant across all metrics as Δ increases, whereas the baseline's utility suffers. The performance of the thresholding variants of the baseline is less predictable. Both the top-0.01% and top-0.001% variants start off with lower utility compared to baseline, which might be due to the fact, when Δ is small, thresholding leaves too few grid cells with non-negative values. On the other hand, the top-0.01% variant's utility also starts to suffer as Δ increases from 256 to 512. This may represent the opposite problem: top-0.01% leaves too many grid cells with noisy positive values, resulting in the decrease in utility.

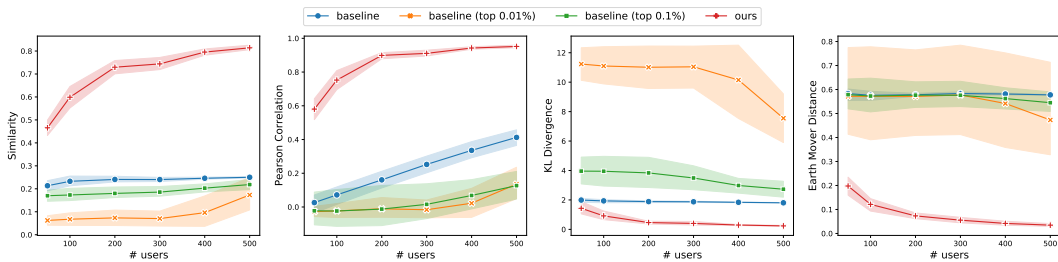


Figure 6: Effect of the # users on different metrics ($\varepsilon = 1$). Shaded areas indicate 95% confidence interval.

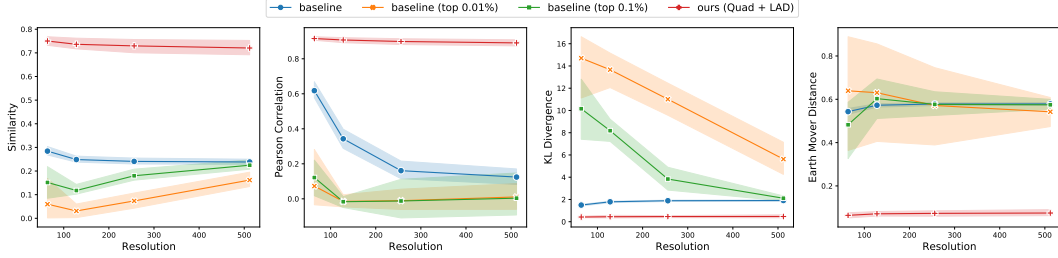


Figure 7: Effect of the resolution on different metrics ($\epsilon = 1$). Shaded areas indicate 95% confidence interval.

We also include the results for similar setups but with privacy parameter $\epsilon = 1$ in Figure 6 and Figure 7. The trends of the vanilla baseline and our algorithm are identical when $\epsilon = 10$. The thresholding variants however have low utility throughout. In fact, for most metrics and parameters, they are worse than the original baseline; it seems plausible that, since the noise is much larger in this case of $\epsilon = 1$, top grid cells kept are mostly noisy and thus the utility is fairly poor.

E.2 Results on the Salicon dataset

We also experiment on the Salicon image saliency dataset [JHDZ15], SALICON, available from <http://salicon.net/>. This dataset is a collection of saliency annotations on the popular Microsoft Common Objects in Context (MS COCO) image database, where each image has 640×480 pixels. For the purposes of our experiment, we assume the data is of the following form: for each (user, image) pair, it consists of a sequence of coordinates in the image where the user looked at.

We repeat the first set of experiments on 38 randomly sampled images (with ≥ 50 users each) from SALICON. The natural images were downsized to a fixed resolution of $\Delta_1 \times \Delta_2 = 320 \times 240$. For each $\epsilon \in \{1, 2, 5, 8, 10, 20\}$, we run our algorithms together with the baseline and its variants on all 38 natural images, with 2 trials for each image. In each trial, we sample a set of 50 users and run all the algorithms; we then compute the metrics between the true heatmap and the estimated heatmap.

The average of these metrics over the 76 runs is presented in Figure 8, together with the 95% confidence interval. As can be seen in the figure, the baseline has rather poor performance across all metrics, even for large $\epsilon = 20$. We experiment with several values of t for the thresholding variant and still observe an advantage of our algorithm consistently across all metrics. We also include examples of the resulting heatmaps with original image overlaid from each approach in Figure 9.

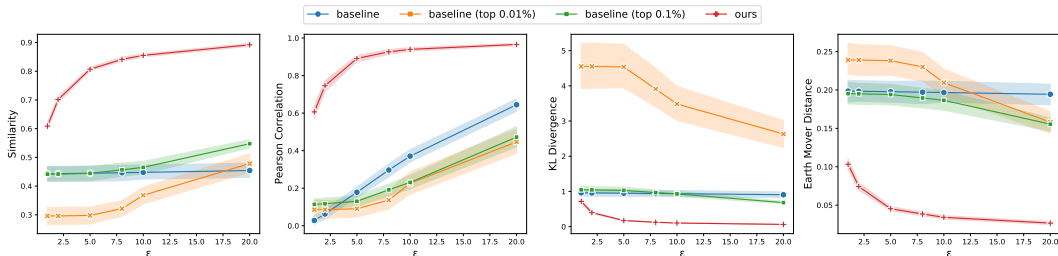


Figure 8: Metrics averaged over 76 runs when varying ϵ . Shaded areas indicate 95% confidence interval.

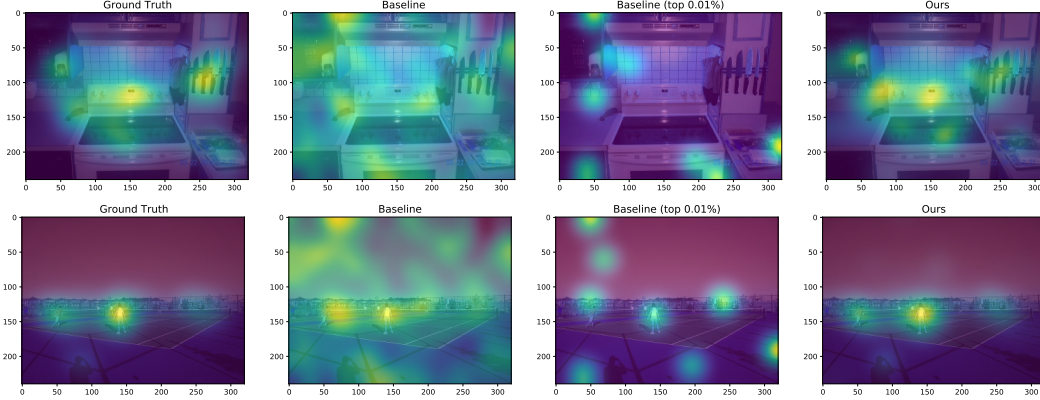


Figure 9: Example visualization of different algorithms for two different natural images from the Salicon dataset (top and bottom rows) for $\varepsilon = 10$ and $n = 50$ users. The algorithms from left to right are: original heatmap (no privacy), baseline, baseline with top 0.01% and our algorithm.

E.3 Results on Synthetic Data

Finally, we experiment on synthetically generated datasets. We generate the data by sampling from a uniform mixture of two-dimensional Gaussian distributions, while the mean and covariance matrix of each Gaussian is randomly generated. The number of Gaussians, their covariances, and the number of samples from the mixture, are changed to control the sparsity of data. Throughout the experiments, we fix the number of users to 200, $\varepsilon = 1$, and use $w = 20$.

We run two sets of experiments to demonstrate the effect of sparsity levels. In the first set of experiments, we fix the number of clusters to 20. We then sample points from this Gaussian mixture until we reach different sparsity values. For each sparsity level, we generate 10 datasets. The experiment results are shown in Figure 10. (Note that we bucketize the sparsity level.)

In the second set of experiments, we vary both the sparsity levels and the number of Gaussians in the mixture. Specifically, we use 5 or 10 Gaussians to produce low sparsity level $< 5\%$, 20 clusters to produce mid-level sparsity like $\sim 15\%$ and $\sim 30\%$, and 80 clusters to produce sparsity level like $\sim 75\%$. The results for this set of experiments are shown in Figure 11.

In both experiments, the rough trends are fairly similar: our algorithm’s utility decreases as the sparsity level increases, whereas the baseline’s utility increases. Upon closer inspection, however, the rate at which our algorithm’s utility decreases is slower when we fixed the number of Gaussians. Indeed, this should be unsurprising: our guarantee is with respect to the best k -sparse approximation (in EMD), which remains roughly constant for the same mixture of Gaussians, regardless of the sparsity. As such, the utility does not decrease too dramatically if we keep the mixture distribution the same. On the other hand, when we also increase the number of Gaussians in the mixture, even the k -sparse approximation fails to capture it well¹⁰, resulting in faster degradation in utility.

F Implementation in Shuffle Model

As alluded to earlier, our algorithm can be easily adapted to any model of DP that supports a “Laplace-like” mechanism. In this section, we illustrate this by giving more details on how to do this in the shuffle model of DP [BEM⁺17, EFM⁺19, CSU⁺19]. Recall that, in the shuffle model, each user produces messages based on

¹⁰Note that while we do not choose k explicitly, it is governed by the parameter w , which we fix to 20 throughout.

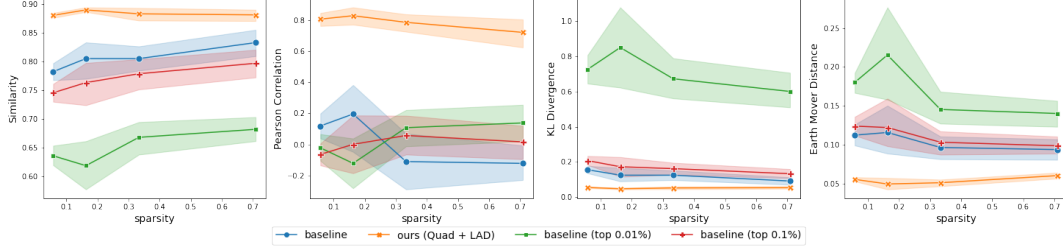


Figure 10: Metrics averaged over 10 runs when varying the sparsity of the dataset; the number of Gaussians in the mixtures is kept constant at 20 respectively. Shaded areas indicate 95% confidence interval.

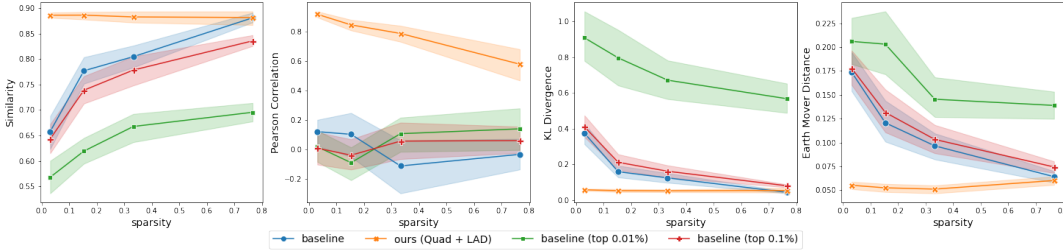


Figure 11: Metrics averaged over 10 runs when varying both the sparsity of the dataset and the number of Gaussians in the mixture; the number of Gaussians is increased from 5 to 10, 20, and 80. Shaded areas indicate 95% confidence interval.

their own input. These messages are then randomly permuted by the shuffler and forwarded to the analyzer, who then computes the desired estimate. The DP guarantee is enforced on the shuffled messages.

To implement our algorithms in the shuffle model, we may use the algorithms of [BBGN20, GMPV20] to compute \mathbf{y}' in Algorithm 1 (instead of running the central DP algorithm); the rest of the steps remain the same. To compute the estimate \mathbf{y}' , the algorithm from [BBGN20] works as follows where $B \in \mathbb{N}$ is a parameter (recall that $\mathbb{Z}_q := \{0, \dots, q-1\}$ and the summation is modulo q):

- Let $q = Bn, m = m_0 + \dots + m_\ell$ and¹¹

$$r = \left\lceil \frac{2 \ln(e^\varepsilon + 1) + 2 \ln(m/\delta) + \ln q}{\ln n} + 1 \right\rceil.$$

- Each user j :
 - Compute $\mathbf{y}^j := [\mathbf{P}_0 \mathbf{p}_j \mathbf{P}_2 \mathbf{p}_j \dots \mathbf{P}_\ell \mathbf{p}_j]$.
 - Scaled & round: $\mathbf{z}^j := \lfloor B \mathbf{y}^j \rfloor$ where the floor is applied coordinate-wise.
 - Add noise:

$$\mathbf{z}'^j := \mathbf{z}^j + \bigotimes_{i \in [\ell]} \text{Polya}(1/n, e^{-\varepsilon_i})^{\otimes m_i}.$$

- Split & Mix: For sample $\mathbf{w}^1, \dots, \mathbf{w}^{r-1}$ i.i.d. at random from \mathbb{Z}_q^m and then let $\mathbf{w}^r = \mathbf{z}^j - \mathbf{w}^1 - \dots - \mathbf{w}^{r-1}$.
- For each $a \in [m]$ and $b \in [r]$, send a tuple (a, w_a^b) to the shuffler¹².
- Once the analyzer receives all the tuples, for each $a \in [m]$, they sum second components of all messages whose first component is a up (over \mathbb{Z}_q), and let the a th coordinate of \mathbf{z}' be equal to the sum. Finally, let $\mathbf{y}' = \mathbf{z}'/B$.

¹¹Note that the parameter is set as in Corollary 6 and Lemma 5.2 of [BBGN20] to achieve (ε, δ) -shuffle DP.

¹²Note that this “coordinate-by-coordinate” technique is from [CSU⁺19].

We note that the Polya distribution and its parameters are set in such a way that the sum of all the noise is exactly the discrete Laplace distribution. Please refer to [BBGN20] for more detail.

Choosing the parameter B will result in a tradeoff between the utility and the communication complexity. For smaller B , the communication will be smaller but there will be more error from rounding. On the other hand, larger B results in larger communication but more accurate simulation of the central DP mechanism. (In fact, as $B \rightarrow \infty$, the resulting estimate \mathbf{y}' converges in distribution to that of the central DP mechanism.)

Empirical Results

We demonstrate the effect of choosing B on communication and utility by running an experiment on the SALICON dataset (where the setup is as in Appendix E.2) with fixed $n = 50$ and $\varepsilon = 5, \delta = 10^{-5}$.

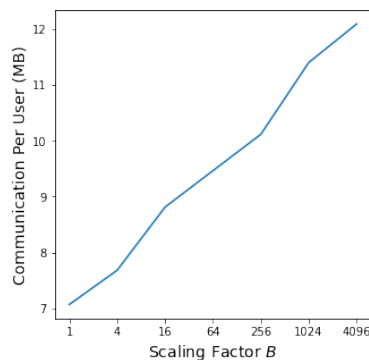


Figure 12: Communication per user in shuffle DP protocol when varying the scaling factor B .

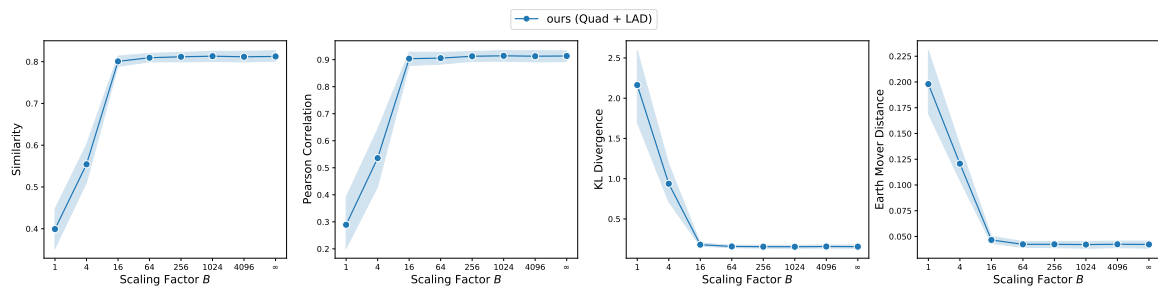


Figure 13: Metrics averaged over 20 runs when varying the scaling factor B . Shaded areas indicate 95% confidence interval. We use the convention $B = \infty$ for the central DP algorithm (which does not apply any rounding).

Communication

We start with the communication. Recall from the aforementioned algorithm that each user sends rm messages, each of length $\lceil \log_2(mq) \rceil$ bits. This gives the total communication per user of $rm \lceil \log_2(mq) \rceil$ bits. The concrete numbers are shown in Figure 12. Note that this is independent of the input datasets, except for the resolution (which effects m). Recall from earlier that we use resolution of 320×240 for the SALICON dataset.

Utility

As for the utility, we run the experiments on the SALICON dataset where the setup is as in Appendix E.2. The utility metrics are reported in Figure 13. In all metrics, the utility is nearly maximized already when B is no more than 256. As per Figure 12, this would correspond to approximately 10MB communication required per user.